

Probing New Physics

with $\bar{B} \rightarrow \rho(770) \ell^- \bar{\nu}_\ell$ and $\bar{B} \rightarrow a_1(1260) \ell^- \bar{\nu}_\ell$

P. Colangelo^a, F. De Fazio^a and F. Loparco^{a,b}

^a Istituto Nazionale di Fisica Nucleare, Sezione di Bari, Via Orabona 4, I-70126 Bari, Italy

^b Università degli Studi di Bari, Via Orabona 4, I-70126 Bari, Italy

Abstract

The B meson semileptonic modes to $\rho(770)$ and $a_1(1260)$ are useful to pin down possible non Standard Model effects. The 4d differential $\bar{B} \rightarrow \rho(\pi\pi)\ell^- \bar{\nu}_\ell$ and $\bar{B} \rightarrow a_1(\rho\pi)\ell^- \bar{\nu}_\ell$ decay distributions are computed in SM and in extensions involving new Lepton Flavour Universality violating semileptonic $b \rightarrow u$ operators. The Large Energy limit for the light meson is also considered for both modes. The new effective couplings are constrained using the available data, and several observables in $\bar{B} \rightarrow \rho(\pi\pi)\ell^- \bar{\nu}_\ell$ in which NP effects can be better identified are selected, using the angular coefficient functions. The complementary role of $\bar{B} \rightarrow \rho(\pi\pi)\ell^- \bar{\nu}_\ell$ and $\bar{B} \rightarrow a_1(\rho\pi)\ell^- \bar{\nu}_\ell$ is discussed.

1 Introduction

The anomalies recently emerged in the flavour sector challenge both the experimental analyses and the theoretical interpretations. In the tree-level $b \rightarrow c\ell^- \bar{\nu}_\ell$ process, deviations of the ratios $R(D^{(*)}) = \frac{\mathcal{B}(B \rightarrow D^{(*)}\tau^- \bar{\nu}_\tau)}{\mathcal{B}(B \rightarrow D^{(*)}\ell^- \bar{\nu}_\ell)}$ (with $\ell = e, \mu$) from the Standard Model (SM) expectations have been observed by BABAR [1, 2], Belle [3–6] and LHCb [7–9]. The measurements can be summarized as $R(D)_{exp} = 0.407 \pm 0.039 \pm 0.024$ to be combined with the new Belle result $R(D)_{exp} = 0.307 \pm 0.037 \pm 0.016$ [10], and $R(D^*)_{exp} = 0.295 \pm 0.011 \pm 0.008$. These measurements are 3.1σ away from the SM values quoted by the Heavy Flavour Averaging Group (HFLAV) [11]: $R(D)_{SM} = 0.299 \pm 0.003$ and $R(D^*)_{SM} = 0.258 \pm 0.005$. The tension, noticed in [12], is significant since the hadronic uncertainties largely cancel out in the ratios of branching fractions [13]. The LHCb measurement $R(J/\psi) = \frac{\mathcal{B}(B_c^+ \rightarrow J/\psi \tau^+ \nu_\tau)}{\mathcal{B}(B_c^+ \rightarrow J/\psi \mu^+ \nu_\mu)} = 0.71 \pm 0.17(\text{stat}) \pm 0.18(\text{syst})$ [14] also exceeds the SM expectation, however in these modes the hadronic uncertainties are sizable [15–17].

Other anomalies have been detected in neutral current $b \rightarrow s$ semileptonic transitions, in the ratios $R_{K^{(*)}} = \frac{\int_{q_{min}^2}^{q_{max}^2} \frac{d\Gamma}{dq^2}(B^+ \rightarrow K^{(*)}\mu^+\mu^-)dq^2}{\int_{q_{min}^2}^{q_{max}^2} \frac{d\Gamma}{dq^2}(B^+ \rightarrow K^{(*)}e^+e^-)dq^2}$ measured by LHCb and Belle. The updated

result for R_K is $R_{K^+} = 0.846^{+0.060}_{-0.054}(\text{stat})^{-0.016}_{-0.014}(\text{syst})$ for $[q_{\min}^2, q_{\max}^2] = [1.1 \text{ GeV}^2, 6 \text{ GeV}^2]$ [18]. For R_{K^*} , the measurements $R_{K^{*0}} = 0.66 \pm_{0.07}^{0.11}(\text{stat}) \pm 0.03(\text{syst})$ for q^2 in $[0.045 \text{ GeV}^2, 1.1 \text{ GeV}^2]$ and $R_{K^{*0}} = 0.69 \pm_{0.07}^{0.11}(\text{stat}) \pm 0.05(\text{syst})$ for q^2 in $[1.1 \text{ GeV}^2, 6 \text{ GeV}^2]$ have been reported by LHCb [19]. Recent Belle measurements, averaged over the neutral and charged modes, are affected by larger errors: $R_{K^*} = 0.52 \pm_{0.26}^{0.36}(\text{stat}) \pm 0.05(\text{syst})$ for q^2 in $[0.045 \text{ GeV}^2, 1.1 \text{ GeV}^2]$, $R_{K^*} = 0.90 \pm_{0.21}^{0.27}(\text{stat}) \pm 0.10(\text{syst})$ for q^2 in $[0.1 \text{ GeV}^2, 8 \text{ GeV}^2]$, and $R_{K^*} = 1.18 \pm_{0.32}^{0.52}(\text{stat}) \pm 0.10(\text{syst})$ for q^2 in $[15 \text{ GeV}^2, 19 \text{ GeV}^2]$ [20]. For all the ratios the SM predictions are close to one.

The anomalies in $b \rightarrow c$ and $b \rightarrow s$ semileptonic modes seem to point to violation of lepton flavour universality (LFU). This accidental SM symmetry is only broken by the Yukawa interactions, while the lepton couplings to the gauge bosons are independent of the lepton flavour.¹ It is unclear if the deviations emerged in angular observables in $B \rightarrow K^* \mu^+ \mu^-$ [22,23] and in the rate of $B_s^0 \rightarrow \phi \mu^+ \mu^-$ [24] can have a connected origin.

In addition to these tensions, the long-standing difference in the determination of the CKM matrix element $|V_{cb}|$ from exclusive modes, in particular $\bar{B} \rightarrow D^* \ell^- \bar{\nu}_\ell$, and from inclusive $\bar{B} \rightarrow X_c \ell^- \bar{\nu}_\ell$ observables (width and moments) still persists in new BABAR [25] and Belle analyses [26], with $|V_{cb}|_{\text{excl}} < |V_{cb}|_{\text{incl}}$. As an alternative to solutions to the puzzle within SM [27–30], a connection has been proposed with the other $b \rightarrow c$ anomalies, within a LFU violating framework [13, 31]. The related experimental signatures have been studied, in particular the 4d differential $\bar{B} \rightarrow D^*(D\pi, D\gamma) \ell^- \bar{\nu}_\ell$ decay distributions for the three lepton species have been scrutinized [32], following analyses that have pointed out the relevance of such distributions [33–36].

It is worth wondering if similar deviations can appear in semileptonic $b \rightarrow u$ transitions. These modes are CKM suppressed with respect to the $b \rightarrow c$ ones, nevertheless high precision measurements are foreseen in the near future by LHCb and Belle II. At present, there is a tension between the exclusive measurement of $|V_{ub}|$, mainly from the $\bar{B} \rightarrow \pi \ell^- \bar{\nu}_\ell$ decay width, and the inclusive determination from $\bar{B} \rightarrow X_u \ell^- \bar{\nu}_\ell$ observables. New information is available on the purely leptonic and on the semileptonic $B \rightarrow \pi$ mode, and analyses within and beyond SM have been carried out [37–45].

Other decay modes can be exploited to pin down deviation from the Standard Model. In particular, for the modes involving the vector $\rho(770)$ and the axial-vector $a_1(1260)$ mesons, the fully differential angular distributions when ρ decays in two pions and a_1 decays into $\rho\pi$ represent an important source of information, due to the wealth of observables that can be analyzed. Such observables are all correlated, and are able to provide coherent patterns within SM and its possible extensions. The different parity of the two mesons acts as a filter for NP operators, which is one of the prime motivations for their consideration. In addition, the $a_1 \rightarrow \rho\pi$ mode has the peculiarity that the longitudinal and transverse ρ polarizations are involved, increasing the plethora of observables on which to focus the experimental analyses. Our NP extension includes lepton-flavour dependent operators, and the comparison with the effects of corresponding $b \rightarrow c$ operators could shed light on the structure of the observed LFU violating effects.

In Sect.2 we introduce the semileptonic $b \rightarrow u$ effective Hamiltonian with the inclusion of new scalar, pseudoscalar, vector and tensor operators weighted by complex couplings. Such

¹For a review on LFU tests see [21].

operators affect the \bar{B} transitions to two leptons and to $\pi\ell\bar{\nu}$, and both channels can be exploited to bound the effective coefficients. In Sect.3 we construct the fully differential decay distributions for the $\bar{B} \rightarrow \rho(\pi\pi)\ell^-\bar{\nu}_\ell$ and $\bar{B} \rightarrow a_1(\rho\pi)\ell^-\bar{\nu}_\ell$ modes, computing the sets of angular coefficient functions in terms of the hadronic matrix elements involved in the transitions. We also consider the Large Energy limit for the light mesons, which allows to express the angular functions in terms of a small number of hadronic form factors. In Sect.4 we analyze several observables in $\bar{B} \rightarrow \rho(\pi\pi)\ell^-\bar{\nu}_\ell$ at a benchmark point in the parameter space of the new couplings, to scrutinize their sensitivity to the different new operators. In particular, we focus on the angular coefficient functions and on combinations for which the new operators would exhibit the largest effect. In Sect.5 we elaborate on the $a_1(1260)$ mode: in such a case the uncertainties on the sets of hadronic form factors are large and still need to be precisely assessed. Nevertheless, we present a numerical analysis of a few observables, to show the sensitivity of the a_1 mode to NP, but the main focus is on the analytic results and on the outcome of the Large Energy limit, to explain the complementarity with the ρ mode. The last Section contains a discussion of the interesting perspectives and the conclusions. In the Appendices we collect the definitions of the hadronic matrix elements and the expressions of the angular coefficient functions for the two modes.

2 Effective $b \rightarrow u\ell^-\bar{\nu}_\ell$ NP Hamiltonian and impact on B meson purely leptonic and semileptonic pion modes

New Physics contributions to beauty hadron decays can be analysed within the Standard Model Effective Field Theory. If the NP scale Λ_{NP} is much larger than the EW scale, all the new massive degrees of freedom can be integrated out, obtaining an effective Hamiltonian in which only the SM fields appear and which is invariant under the SM gauge group. This Hamiltonian contains additional operators with respect to SM, suppressed by increasing powers of Λ_{NP} . The contribution $\mathcal{O}\left(\frac{1}{\Lambda_{NP}^2}\right)$ includes dimension-six four-fermion operators [46].

To describe the modes $\bar{B} \rightarrow M_u\ell^-\bar{\nu}_\ell$ with M_u a light meson comprising an up quark we consider the effective Hamiltonian

$$H_{\text{eff}}^{b \rightarrow u\ell\nu} = \frac{G_F}{\sqrt{2}} V_{ub} \left\{ (1 + \epsilon_V^\ell) (\bar{u}\gamma_\mu(1 - \gamma_5)b) (\bar{\ell}\gamma^\mu(1 - \gamma_5)\nu_\ell) \right. \\ + \epsilon_S^\ell (\bar{u}b) (\bar{\ell}(1 - \gamma_5)\nu_\ell) + \epsilon_P^\ell (\bar{u}\gamma_5 b) (\bar{\ell}(1 - \gamma_5)\nu_\ell) \\ \left. + \epsilon_T^\ell (\bar{u}\sigma_{\mu\nu}(1 - \gamma_5)b) (\bar{\ell}\sigma^{\mu\nu}(1 - \gamma_5)\nu_\ell) \right\} + h.c. , \quad (1)$$

consisting in the SM term and in NP terms weighted by complex lepton-flavour dependent couplings $\epsilon_{V,S,P,T}^\ell$. V_{ub} and ϵ_V^ℓ are independent parameters, since the product $V_{ub}(1 + \epsilon_V^\ell)$ is not a mere redefinition of the SM V_{ub} . We assume a purely left-handed lepton current as in SM, an extensively probed structure. We exclude the quark right-handed vector current, since the only four-fermion operator of this type, invariant under the SM group, is non-linear in the Higgs field [47–49]².

²Right-handed currents are investigated in [38, 39, 41].

The couplings of the NP operators in (1) are constrained by the measurements, in particular on the purely leptonic B^- and semileptonic $\bar{B} \rightarrow \pi\ell^-\bar{\nu}_\ell$ channels. Indeed, the $B^- \rightarrow \ell^-\bar{\nu}_\ell$ decay width obtained from $H_{\text{eff}}^{b \rightarrow u\ell\nu}$ in Eq.(1) reads

$$\Gamma(B^- \rightarrow \ell^-\bar{\nu}_\ell) = \frac{G_F^2 |V_{ub}|^2 f_B^2 m_B^3}{8\pi} \left(1 - \frac{m_\ell^2}{m_B^2}\right)^2 \left| \left(\frac{m_\ell}{m_B}\right) (1 + \epsilon_V^\ell) + \frac{m_B}{m_b + m_u} \epsilon_P^\ell \right|^2, \quad (2)$$

with the decay constant f_B defined as

$$\langle 0 | \bar{u} \gamma_\mu \gamma_5 b | \bar{B}(p) \rangle = i f_B p_\mu. \quad (3)$$

The ew correction to (2) is tiny. This mode is insensitive to the NP scalar and tensor operators. The pseudoscalar operator removes the helicity suppression, which is effective for light leptons, with a consequent stringent constraint for the effective couplings $\epsilon_P^{\ell,\mu}$.

The semileptonic $\bar{B} \rightarrow \pi\ell^-\bar{\nu}_\ell$ decay distribution in the dilepton mass squared q^2 , obtained from Eq.(1) parametrizing the weak matrix element in terms of the form factors $f_i(q^2) = f_i^{B \rightarrow \pi}(q^2)$ as in Appendix A, is:

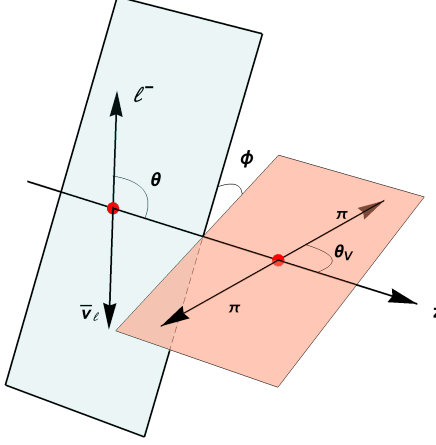
$$\begin{aligned} \frac{d\Gamma}{dq^2}(\bar{B} \rightarrow \pi\ell^-\bar{\nu}_\ell) &= \frac{G_F^2 |V_{ub}|^2 \lambda^{1/2}(m_B^2, m_\pi^2, q^2)}{128 m_B^3 \pi^3 q^2} \left(1 - \frac{m_\ell^2}{q^2}\right)^2 \\ &\times \left\{ \left| m_\ell(1 + \epsilon_V^\ell) + \frac{q^2 \epsilon_S^\ell}{m_b - m_u} \right|^2 (m_B^2 - m_\pi^2)^2 f_0^2(q^2) + \right. \\ &+ \lambda(m_B^2, m_\pi^2, q^2) \left[\frac{1}{3} \left| m_\ell(1 + \epsilon_V^\ell) f_+(q^2) + \frac{4q^2}{m_B + m_\pi} \epsilon_T^\ell f_T(q^2) \right|^2 \right. \\ &\left. \left. + \frac{2q^2}{3} \left| (1 + \epsilon_V^\ell) f_+(q^2) + 4 \frac{m_\ell}{m_B + m_\pi} \epsilon_T^\ell f_T(q^2) \right|^2 \right] \right\}, \quad (4) \end{aligned}$$

with λ the triangular function. In this case the pseudoscalar operator does not contribute.

As in the Hamiltonian (1), in Eqs.(2) and (4) the CKM matrix element V_{ub} appears in the combination $V_{ub}(1 + \epsilon_V^\ell)$. The lepton-flavour dependence of the effective couplings would manifest in different determinations of V_{ub} from channels involving different lepton species. We discuss below how the experimental measurements constrain the parameter spaces.

Continuing with the semileptonic mode to pion, in the large energy limit of the emitted pion, using Eq.(A.13) for the weak matrix element, the decay distribution is expressed in terms of a single form factor ξ_π [50, 51]:

$$\begin{aligned} \frac{d\Gamma}{dE}(\bar{B} \rightarrow \pi\ell^-\bar{\nu}_\ell) &= \frac{G_F^2 |V_{ub}|^2 \lambda^{1/2}(m_B^2, m_\pi^2, q^2)}{64 m_B^2 \pi^3 q^2} \left(1 - \frac{m_\ell^2}{q^2}\right)^2 \xi_\pi^2(E) \\ &\times \left\{ \left| m_\ell(1 + \epsilon_V^\ell) + \frac{q^2 \epsilon_S^\ell}{m_b - m_u} \right|^2 (m_B^2 - m_\pi^2)^2 \left(\frac{m_B^2 + m_\pi^2 - q^2}{m_B^2} \right)^2 \right. \\ &\left. + \lambda(m_B^2, m_\pi^2, q^2) \left[\frac{1}{3} \left| m_\ell(1 + \epsilon_V^\ell) + \frac{4q^2}{m_B} \epsilon_T^\ell \right|^2 + \frac{2q^2}{3} \left| (1 + \epsilon_V^\ell) + \frac{4m_\ell}{m_B} \epsilon_T^\ell \right|^2 \right] \right\}, \quad (5) \end{aligned}$$

Figure 1: Kinematics of the decay mode $\bar{B} \rightarrow \rho(\pi\pi)\ell^-\bar{\nu}_\ell$.

with $q^2 = m_B^2 + m_\pi^2 - 2m_BE$. While the full kinematical range for E is $m_\pi \leq E \leq \frac{m_B}{2} \left(1 + \frac{m_\pi^2}{m_B^2} - \frac{m_\ell^2}{m_B^2}\right)$, Eq.(5) only holds for large $E \simeq \frac{m_B}{2}$. This expression is useful if the distribution is independently measured for the three charged leptons, since the ratios

$$\frac{dR(\pi)^{\ell\ell'}}{dE} = \frac{d\Gamma}{dE}(\bar{B} \rightarrow \pi\ell^-\bar{\nu}_\ell) / \frac{d\Gamma}{dE}(\bar{B} \rightarrow \pi\ell'^-\bar{\nu}_{\ell'}) \quad (6)$$

are free of hadronic uncertainties in this limit, and only involve combinations of the lepton flavour-dependent couplings $\epsilon_{V,S,T}^{\ell,\ell'}$.

3 Fully differential angular distributions for $\bar{B} \rightarrow \rho(\rightarrow \pi\pi)\ell^-\bar{\nu}_\ell$ and $\bar{B} \rightarrow a_1(\rightarrow \rho\pi)\ell^-\bar{\nu}_\ell$

The main sensitivity to the new operators in (1), in the modes $\bar{B} \rightarrow \rho(\rightarrow \pi\pi)\ell^-\bar{\nu}_\ell$ and $\bar{B} \rightarrow a_1(\rightarrow \rho\pi)\ell^-\bar{\nu}_\ell$, is in the 4d differential decay distribution in the variables q^2 and in the angles θ , θ_V and ϕ described in Fig.1. For the ρ mode the distribution is written as ³:

$$\begin{aligned} \frac{d^4\Gamma(\bar{B} \rightarrow \rho(\rightarrow \pi\pi)\ell^-\bar{\nu}_\ell)}{dq^2 d\cos\theta d\phi d\cos\theta_V} &= \mathcal{N}_\rho |\vec{p}_\rho| \left(1 - \frac{m_\ell^2}{q^2}\right)^2 \left\{ I_{1s}^\rho \sin^2\theta_V + I_{1c}^\rho \cos^2\theta_V \right. \\ &+ (I_{2s}^\rho \sin^2\theta_V + I_{2c}^\rho \cos^2\theta_V) \cos 2\theta \\ &+ I_3^\rho \sin^2\theta_V \sin^2\theta \cos 2\phi + I_4^\rho \sin 2\theta_V \sin 2\theta \cos \phi \\ &+ I_5^\rho \sin 2\theta_V \sin \theta \cos \phi + (I_{6s}^\rho \sin^2\theta_V + I_{6c}^\rho \cos^2\theta_V) \cos \theta \\ &\left. + I_7^\rho \sin 2\theta_V \sin \theta \sin \phi \right\}, \end{aligned} \quad (7)$$

³Other angular structures appear in the differential distributions if a quark right-handed vector current is included in Eq.(1).

with $\mathcal{N}_\rho = \frac{3G_F^2|V_{ub}|^2\mathcal{B}(\rho \rightarrow \pi\pi)}{128(2\pi)^4m_B^2}$. This expression, together with the relation of the coefficient functions to the hadronic matrix elements, has been computed in the narrow width approximation, resulting in a factorization of the production and decay amplitude of the intermediate vector meson. The factorization is connected to the procedure adopted in the experimental analyses to select the contributions of the intermediate resonances [52].⁴ A $\pi\pi$ contribution considered as an improvement of the narrow width approximation has been investigated through the computation of the $B \rightarrow \pi\pi$ matrix elements in the kinematical regime of small dipion invariant mass and large energy, concluding that it represents a small effect [56–58].

For the $a_1(\rho\pi)$ channel it is useful to provide the expressions for the modes where the final ρ is transversely (ρ_\perp) or longitudinally (ρ_\parallel) polarized, as specified in Appendix B. The expression of the 4d distribution amplitude is:

$$\begin{aligned} \frac{d^4\Gamma(\bar{B} \rightarrow a_1(\rightarrow \rho_{\parallel(\perp)}\pi)\ell^-\bar{\nu}_\ell)}{dq^2 d\cos\theta d\phi d\cos\theta_V} &= \mathcal{N}_{a_1}^{\parallel(\perp)} |\vec{p}_{a_1}| \left(1 - \frac{m_\ell^2}{q^2}\right)^2 \left\{ I_{1s,\parallel(\perp)}^{a_1} \sin^2\theta_V + I_{1c,\parallel(\perp)}^{a_1} (3 + \cos 2\theta_V) \right. \\ &+ \left(I_{2s,\parallel(\perp)}^{a_1} \sin^2\theta_V + I_{2c,\parallel(\perp)}^{a_1} (3 + \cos 2\theta_V) \right) \cos 2\theta \\ &+ I_{3,\parallel(\perp)}^{a_1} \sin^2\theta_V \sin^2\theta \cos 2\phi + I_{4,\parallel(\perp)}^{a_1} \sin 2\theta_V \sin 2\theta \cos \phi \\ &+ I_{5,\parallel(\perp)}^{a_1} \sin 2\theta_V \sin \theta \cos \phi \\ &+ \left(I_{6s,\parallel(\perp)}^{a_1} \sin^2\theta_V + I_{6c,\parallel(\perp)}^{a_1} (3 + \cos 2\theta_V) \right) \cos \theta \\ &\left. + I_{7,\parallel(\perp)}^{a_1} \sin 2\theta_V \sin \theta \sin \phi \right\}, \end{aligned} \quad (8)$$

with the subscripts \perp, \parallel referring to the two ρ polarizations. The coefficients $\mathcal{N}_{a_1}^{\parallel(\perp)}$ read: $\mathcal{N}_{a_1}^{\parallel(\perp)} = \frac{3G_F^2|V_{ub}|^2\mathcal{B}(a_1 \rightarrow \rho_{\parallel(\perp)}\pi)}{128(2\pi)^4m_B^2}$. The separation of the ρ polarizations is an experimental challenge, which is justified in view of the different sensitivity of the angular coefficient functions to the NP operators. The unpolarized case is recovered combining the expressions for the transverse and longitudinal ρ polarization. The NWA has been adopted also for the computation of the distribution (8) with the derivation of the relations of the angular coefficient functions in terms of $B \rightarrow a_1$ matrix elements. This is a more debatable procedure than for the ρ channel. Its motivation relies on the assumption that the experimental analyses can constrain the $\rho\pi$ invariant mass in a narrow range around the a_1 peak, separating the production and decay process of the intermediate resonance. Going beyond such a limit would require to consider the $\rho\pi$ invariant mass distribution, with the $B \rightarrow a_1$ form factors extrapolated to different values of such a mass, with uncontrolled uncertainties. On the other hand, considering the three pion final state would include contributions from several resonances of various spin-parity, affected in different ways from the NP operators when produced in semileptonic B modes.

⁴Studies of the $B_{\ell 4}$ mode are in [53–55].

The angular coefficient functions I_i^ρ and $I_i^{a_1}$ in Eqs.(7) and (8) can be written as

$$\begin{aligned} I_i &= |1 + \epsilon_V|^2 I_i^{SM} + |\epsilon_X|^2 I_i^{NP,X} + |\epsilon_T|^2 I_i^{NP,T} + 2 \operatorname{Re} [\epsilon_X(1 + \epsilon_V^*)] I_i^{INT,X} \\ &\quad + 2 \operatorname{Re} [\epsilon_T(1 + \epsilon_V^*)] I_i^{INT,T} + 2 \operatorname{Re} [\epsilon_X \epsilon_T^*] I_i^{INT,XT}, \quad (i = 1, \dots, 6), \quad (9) \\ I_7 &= 2 \operatorname{Im} [\epsilon_X(1 + \epsilon_V^*)] I_7^{INT,X} + 2 \operatorname{Im} [\epsilon_T(1 + \epsilon_V^*)] I_7^{INT,T} + 2 \operatorname{Im} [\epsilon_X \epsilon_T^*] I_7^{INT,XT}, \end{aligned}$$

with $X = P$ in case of ρ , and $X = S$ in case of a_1 . The coefficient functions I_i^{SM} , I_i^{NP} and I_i^{INT} , expressed in terms of helicity amplitudes, are collected in Tables 2-9 of Appendix B, together with the relations of the helicity amplitudes to the hadron form factors.

Examining the angular coefficient functions and their expressions, several remarks are in order.

- 1) With the exception of I_7 , all angular coefficient functions do not vanish in SM and are sensitive to ϵ_V . Apart from such a dependence, we can identify structures useful to disentangle the effects of the other S, P and T operators. In $B \rightarrow \rho\ell\bar{\nu}_\ell$ the functions I_{1s}^ρ , I_{2s}^ρ , I_{2c}^ρ , I_3^ρ , I_4^ρ , I_{6s}^ρ do not depend on ϵ_P , as it can be inferred from Table 3, and are sensitive only to the tensor operator. We denote these structures as belonging to set A, while set B comprises the remaining ones. An analogous situation occurs for the corresponding quantities in $B \rightarrow a_1(\rho\parallel\pi)\ell\bar{\nu}_\ell$, which do not depend on ϵ_S (Table 6), while in $B \rightarrow a_1(\rho_\perp\pi)\ell\bar{\nu}_\ell$ the functions $I_{1c,\perp}^{a_1}$, $I_{2s,\perp}^{a_1}$, $I_{2c,\perp}^{a_1}$, $I_{3,\perp}^{a_1}$, $I_{4,\perp}^{a_1}$, $I_{6c,\perp}^{a_1}$ are insensitive to the scalar operator (Table 7).
- 2) In the absence of the tensor operator, the ρ and a_1 modes give complementary information on the pseudoscalar P (in the ρ channel) and scalar S (in a_1) operators, together with the purely leptonic mode (sensitive to P) and $B \rightarrow \pi$ mode (sensitive to S).
- 3) There are angular coefficient functions that depend only on the helicity amplitudes H_\pm , not on H_0 and H_t . These affect observables corresponding to the transversely polarized W , hence to transverse ρ in $B \rightarrow \rho\ell\bar{\nu}_\ell$ and transverse a_1 in $B \rightarrow a_1\ell\bar{\nu}_\ell$. Such observables depend on ϵ_T , not on ϵ_P (in the ρ mode) or ϵ_S (in the a_1 mode).
- 4) In the Large Energy Limit of the light meson, the form factors parametrizing the $B \rightarrow \rho(a_1)$ weak matrix elements can be written in terms of two form factors, $\xi_\perp^\rho(\xi_\perp^{a_1})$ and $\xi_\parallel^\rho(\xi_\parallel^{a_1})$ defined by the relations (A.14), (A.15). In this limit, several angular coefficients depend only on the form factor ξ_\perp , others involve both ξ_\perp and ξ_\parallel . The coefficients depending only on $\xi_\perp^{\rho,a_1}(E)$ are:
 - in $B \rightarrow \rho(770)$ mode: I_{1s}^ρ , I_{2s}^ρ , I_3^ρ and I_{6s}^ρ ,
 - in $B \rightarrow a_1(1260)$ mode:
 - for final ρ longitudinally polarized, $I_{1s,\parallel}^{a_1}$, $I_{2s,\parallel}^{a_1}$, $I_{3,\parallel}^{a_1}$ and $I_{6s,\parallel}^{a_1}$,
 - for ρ transversely polarized, $I_{1c,\perp}^{a_1}$, $I_{2c,\perp}^{a_1}$, $I_{3,\perp}^{a_1}$ and $I_{6c,\perp}^{a_1}$.

When a single form factor is involved, ratios of coefficient functions are free of hadronic uncertainties (in the Large Energy Limit).

The conclusion is that, measuring the differential angular distribution and reconstructing the angular coefficient functions, it is possible to define sets of observables particularly sensitive to different NP terms in (1). This would allow to determine the new couplings ϵ_i^ℓ and carry out tests, e.g., of LFU, comparing results obtained in the μ and τ modes.

4 Constraints on the effective couplings and $\bar{B} \rightarrow \rho \ell^- \bar{\nu}_\ell$ observables

We want to present examples of the possible effects of the NP operators in (1) in $\bar{B} \rightarrow \rho \ell^- \bar{\nu}_\ell$, identifying the most sensitive observables. For that, we constrain the space of the new couplings using the available data and a set of hadronic quantities. More precise experimental measurements or more accurate theoretical determinations of the hadronic quantities, when available in the future, will modify the ranges of the couplings, but the strategy and the overall picture we are presenting will remain valid.

The couplings ϵ_V^μ , ϵ_P^μ , ϵ_T^μ are constrained by the measurements $\mathcal{B}(\bar{B}^0 \rightarrow \pi^+ \ell^- \bar{\nu}_\ell) = (1.50 \pm 0.06) \times 10^{-4}$ and $\mathcal{B}(\bar{B}^0 \rightarrow \rho^+ \ell^- \bar{\nu}_\ell) = (2.94 \pm 0.21) \times 10^{-4}$ [59], together with $\mathcal{B}(B^- \rightarrow \mu^- \bar{\nu}_\mu) = (6.46 \pm 2.2 \pm 1.60) \times 10^{-7}$ (and 90% probability interval $[2.0, 10.7] \times 10^{-7}$) [60]. For e and τ , the results for the purely leptonic modes are $\mathcal{B}(B^- \rightarrow e^- \bar{\nu}_e) < 9.8 \times 10^{-7}$ and $\mathcal{B}(B^- \rightarrow \tau^- \bar{\nu}_\tau) = (1.09 \pm 0.24) \times 10^{-4}$ [59]. The upper bound $\mathcal{B}(\bar{B}^0 \rightarrow \pi^+ \tau^- \bar{\nu}_\tau) < 2.5 \times 10^{-4}$ has also been established [61]. We use the $B \rightarrow \pi$ form factors given in Appendix C, obtained interpolating the Light-Cone sum rule results at low q^2 computed in Refs. [62, 63] with the lattice QCD results at large values of q^2 averaged by HFLAG [64]. For the $B \rightarrow \rho$ transition we use the form factors in Ref. [65], which update previous Light-Cone sum rule computations [66] and extrapolate the low q^2 determination to the full kinematical range.

In the case of μ , the parameter space for the NP couplings, displayed in Fig.2, is found imposing that the purely leptonic BR is in the range $[2.0, 10.7] \times 10^{-7}$, and that the semileptonic $\bar{B} \rightarrow \pi$ and $\bar{B} \rightarrow \rho$ branching fractions are compatible within 2σ with measurement. The benchmark point shown in Fig.2 is chosen in the region of the smallest

$$\chi^2 = \sum_i^3 \left(\frac{\mathcal{B}_i^{th} - \mathcal{B}_i^{exp}}{\Delta \mathcal{B}_i^{exp}} \right)^2 \quad (10)$$

for the three modes, varying $|V_{ub}|$ in $[3.5, 4.4] \times 10^{-3}$. Specifically, in the region of smallest χ^2 we have selected the points in the parameter space having $\epsilon_V^\ell = 0$ and all the other $\epsilon_A^\ell \neq 0$, with $A = S, P, T$. Our benchmark point is the one minimizing χ^2 . We set $\epsilon_V^\ell = 0$ to maximize the sensitivity to the other NP couplings.

For the τ modes, due to the smaller number of experimental constraints, we consider a limited parameter space setting $\epsilon_V^\tau = 0$ and $\epsilon_S^\tau = 0$ from the beginning. The region for ϵ_P^τ in Fig.3 (left panel) is constrained imposing the compatibility of $\mathcal{B}(B^- \rightarrow \tau^- \bar{\nu}_\tau)$ with measurement. We have checked that $\frac{\mathcal{B}(B^- \rightarrow \mu^- \bar{\nu}_\mu)}{\mathcal{B}(B^- \rightarrow \tau^- \bar{\nu}_\tau)}$ lies within the experimental range when ϵ_V^μ , ϵ_P^μ are varied in their ranges. The region for ϵ_T^τ (right panel) is obtained imposing the experimental upper bound for $\mathcal{B}(\bar{B}^0 \rightarrow \pi^+ \tau^- \bar{\nu}_\tau)$ together with the limit for $R_\pi = \frac{\mathcal{B}(\bar{B}^0 \rightarrow \pi^+ \tau^- \bar{\nu}_\tau)}{\mathcal{B}(\bar{B}^0 \rightarrow \pi^+ \mu^- \bar{\nu}_\mu)}$. In

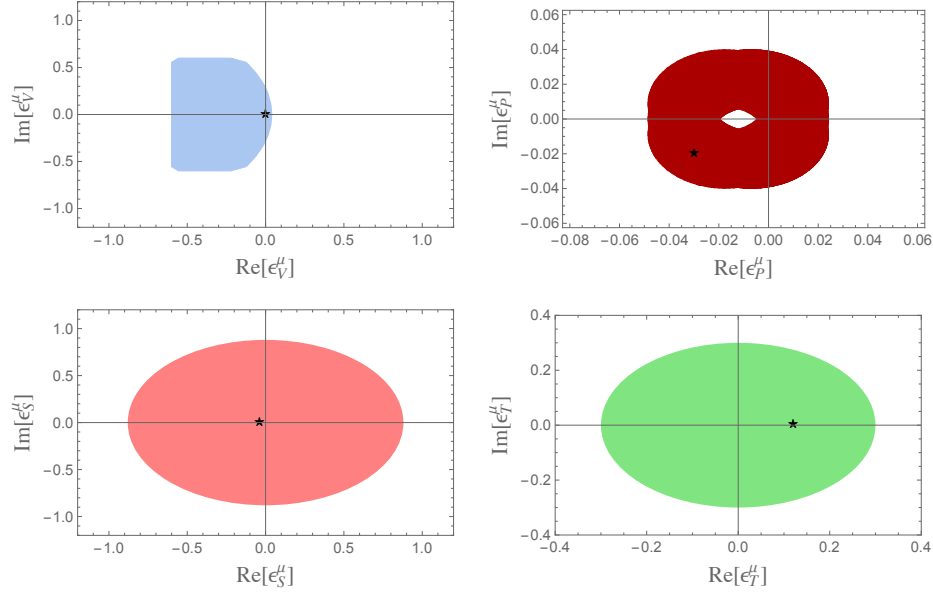


Figure 2: Allowed regions for the couplings ϵ_V^μ , ϵ_P^μ , ϵ_S^μ and ϵ_T^μ . The colors distinguish the various couplings. The stars correspond to the benchmark points, chosen in the region of minimum χ^2 : $(\text{Re}[\epsilon_V^\mu], \text{Im}[\epsilon_V^\mu]) = (0, 0)$, $(\text{Re}[\epsilon_P^\mu], \text{Im}[\epsilon_P^\mu]) = (-0.03, -0.02)$, $(\text{Re}[\epsilon_T^\mu], \text{Im}[\epsilon_T^\mu]) = (0.12, 0)$ and $(\text{Re}[\epsilon_S^\mu], \text{Im}[\epsilon_S^\mu]) = (-0.04, 0)$, with $|V_{ub}| = 3.5 \times 10^{-3}$.

the wide resulting region we set the range for ϵ_T^τ , with the parameters for the muon fixed at their benchmark values, then we fix a benchmark point to provide an example of NP effects.

We can now compare observables in SM and NP. The angular coefficient functions I_{1s}^ρ , I_{2s}^ρ , I_{2c}^ρ , I_3^ρ , I_4^ρ and I_{6s}^ρ , independent of ϵ_P , are shown in Fig.4, setting ϵ_T^μ at benchmark point. The zero in $I_{2s}^\rho(q^2)$ is absent in SM and appears in NP. The other coefficient functions are drawn

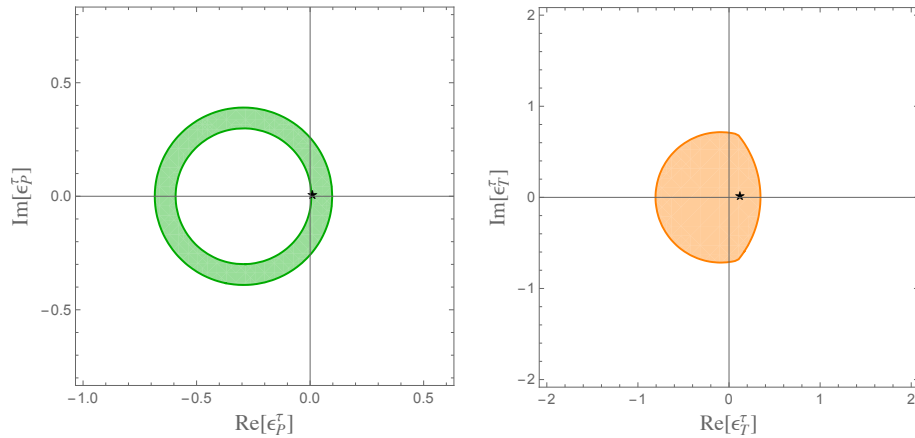


Figure 3: Allowed regions for the couplings ϵ_P^τ and ϵ_T^τ . The stars correspond to the benchmark points chosen setting $\epsilon_V^\tau = 0$ and $\epsilon_S^\tau = 0$: $(\text{Re}[\epsilon_P^\tau], \text{Im}[\epsilon_P^\tau]) = (0.01, 0)$ and $(\text{Re}[\epsilon_T^\tau], \text{Im}[\epsilon_T^\tau]) = (0.12, 0)$.

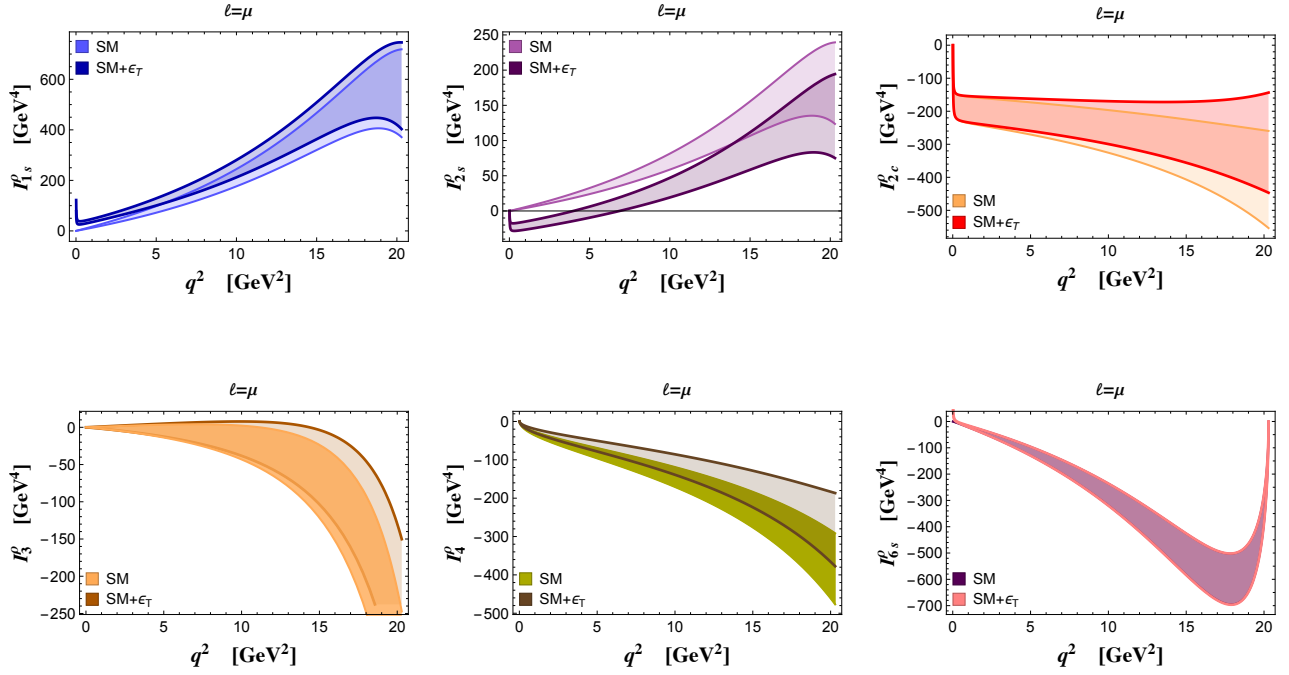


Figure 4: $\bar{B} \rightarrow \rho(\pi\pi) \mu^- \bar{\nu}_\mu$ mode: angular coefficient functions $I_i^\rho(q^2)$ in set A, for SM and NP at the benchmark point. A zero in $I_{2s}^\rho(q^2)$ appears in NP.

in Fig.5, and also in this case there is a zero in $I_{6c}^\rho(q^2)$ which is absent in SM. The function I_7^ρ vanishes in SM, and is only sensitive to the imaginary part of the NP couplings; it is shown in Fig.6. The angular functions for the τ modes are in Fig.7 and 8; I_7^ρ vanishes since at the chosen benchmark point all the NP couplings ϵ^τ are real. Also in this mode the coefficient I_{6c}^ρ has a zero not appearing in SM.

The measurement of the angular coefficients functions allows to determine the new cou-

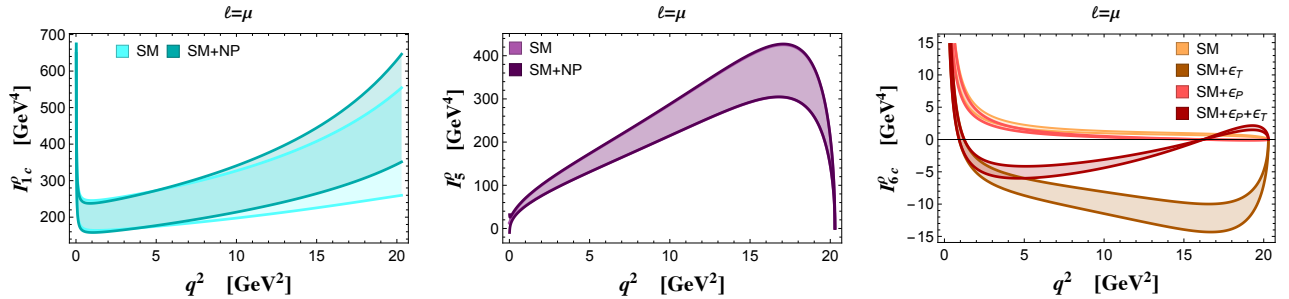


Figure 5: $\bar{B} \rightarrow \rho(\pi\pi) \mu^- \bar{\nu}_\mu$ mode: angular coefficient functions (set B) $I_{1c}^\rho(q^2)$ (left), $I_5^\rho(q^2)$ (middle) and $I_{6c}^\rho(q^2)$ (right) for SM and NP at the benchmark point.

plings. Let us consider the ratios

$$R_{2s/1s}^\rho(q^2) = \frac{I_{2s}^\rho(q^2)}{I_{1s}^\rho(q^2)}, \quad (11)$$

$$R_{2s/1s}^{a_1, \parallel}(q^2) = \frac{I_{2s, \parallel}^{a_1}(q^2)}{I_{1s, \parallel}^{a_1}(q^2)}, \quad (12)$$

and $R_{2s/1s}^{a_1, \parallel} = R_{2c/1c}^{a_1, \perp}$. In SM $R_{2s/1s}^\rho$ is form factor independent. In NP it is still form factor independent in the Large Energy limit, where I_{2s}^ρ and I_{1s}^ρ depend on ξ_\perp^ρ . As shown in Fig.9, the ratio (11) has a zero in the NP, not in SM, whose position $q_{0, \rho}^2$ has a weak form factor effect and depends only on $|\epsilon_T^\mu|$. In the Large Energy Limit we have

$$|\epsilon_T^\mu|^2 = \frac{q_{0, \rho}^2}{16m_B^2} \frac{\lambda(m_B^2, m_\rho^2, q_{0, \rho}^2) + 2m_B^2 m_\rho^2}{\lambda(m_B^2, m_\rho^2, q_{0, \rho}^2) + 2q_{0, \rho}^2 m_\rho^2}. \quad (13)$$

Analogously, for the $(a_1)_\parallel$ mode (and for $(a_1)_\perp$ considering $R_{2c/1c}$) we have:

$$|\epsilon_T^\mu|^2 = \frac{q_{0, a_1}^2}{16m_B^2} \frac{\lambda(m_B^2, m_{a_1}^2, q_{0, a_1}^2) + 2m_B^2 m_{a_1}^2}{\lambda(m_B^2, m_{a_1}^2, q_{0, a_1}^2) + 2q_{0, a_1}^2 m_{a_1}^2}. \quad (14)$$

The positions of the zeros in two modes are related, see Fig.10, and their independent measurement would provide a connection with the tensor operator.

Another suitable quantity is the angular coefficient function I_{6c}^ρ shown in the right panel of Fig.5 in SM and NP, which is sensitive to ϵ_V , ϵ_P , ϵ_T . At our benchmark point $\epsilon_V \simeq 0$, hence we keep only the ϵ_P and ϵ_T dependence:

$$(I_{6c}^\rho)_{|\epsilon_V \simeq 0} = (-2H_t^\rho) \left[4H_0^\rho m_\ell^2 - \text{Re}[\epsilon_T] H_L^{NP, \rho} m_\ell \sqrt{q^2} + 4\text{Re}[\epsilon_P] H_0^\rho \frac{m_\ell}{m_b + m_u} q^2 - H_L^{NP, \rho} \text{Re}[\epsilon_P \epsilon_T^*] \frac{(q^2)^{3/2}}{m_b + m_u} \right]. \quad (15)$$

Considering the q^2 -dependence of the helicity amplitudes in Appendix B, we have the following possibilities:

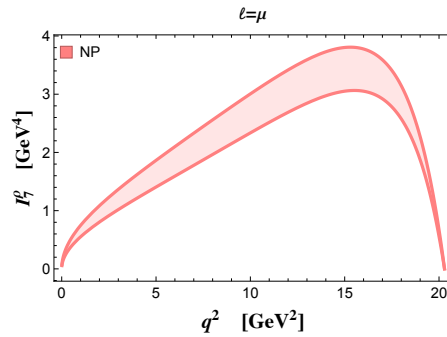


Figure 6: $\bar{B} \rightarrow \rho(\pi\pi) \mu^- \bar{\nu}_\mu$ mode: angular coefficient function $I_7^\rho(q^2)$ in NP with the pseudoscalar operator at the benchmark point.

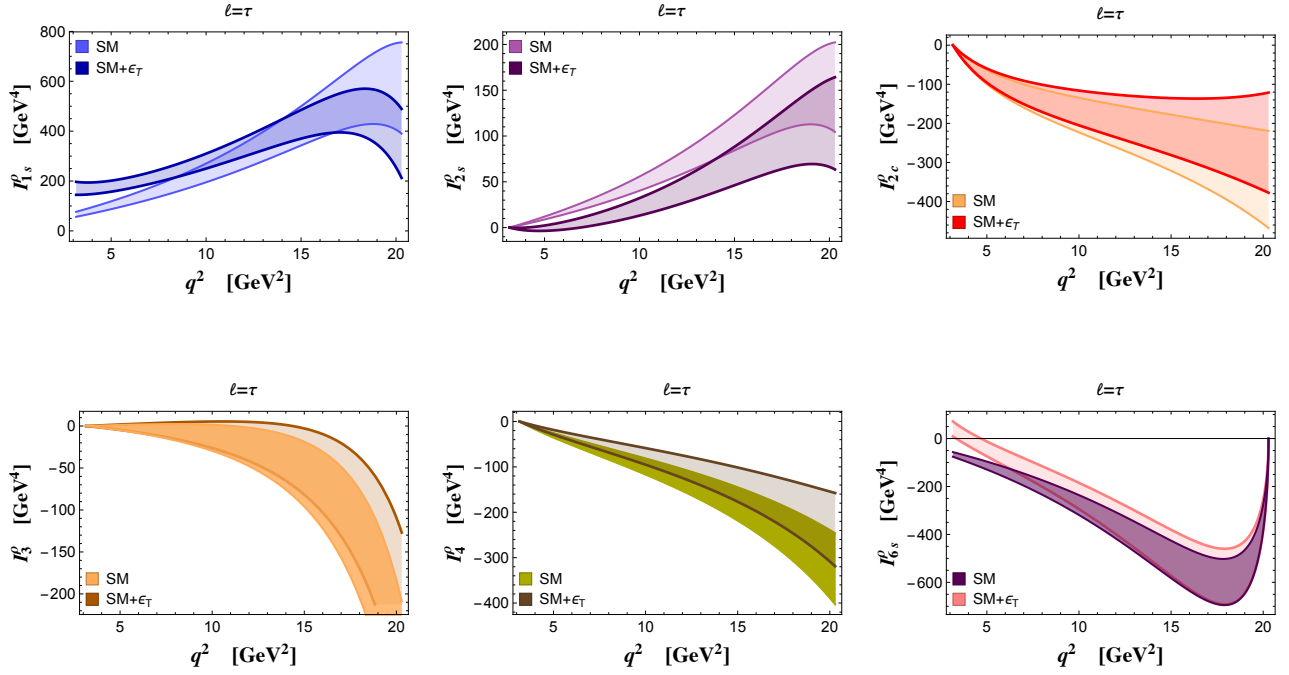


Figure 7: $\bar{B} \rightarrow \rho(\pi\pi) \tau^- \bar{\nu}_\tau$ mode: angular coefficient functions $I_i^\rho(q^2)$ in set A for SM and NP at the benchmark point.

- No NP, i.e. $\epsilon_P = \epsilon_T = 0$. In this case, $I_{6c}^\rho = -8H_t^\rho H_0^\rho m_\ell^2$ does not have a zero, as shown in Fig.5 (right panel).
- NP with $\epsilon_T = 0$ and $\epsilon_P \neq 0$. This gives:

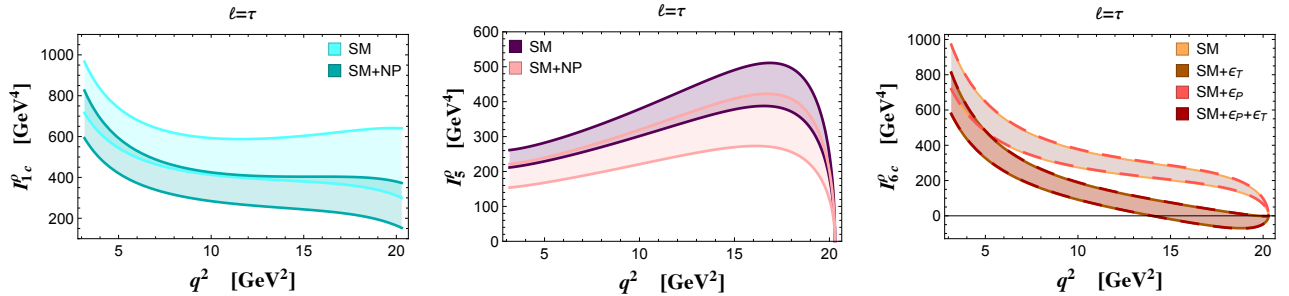


Figure 8: $\bar{B} \rightarrow \rho(\pi\pi) \tau^- \bar{\nu}_\tau$ mode: angular coefficient functions (set B) $I_{1c}^\rho(q^2)$ (left), $I_5^\rho(q^2)$ (middle) and $I_{6c}^\rho(q^2)$ (right) for SM and NP at the benchmark point.

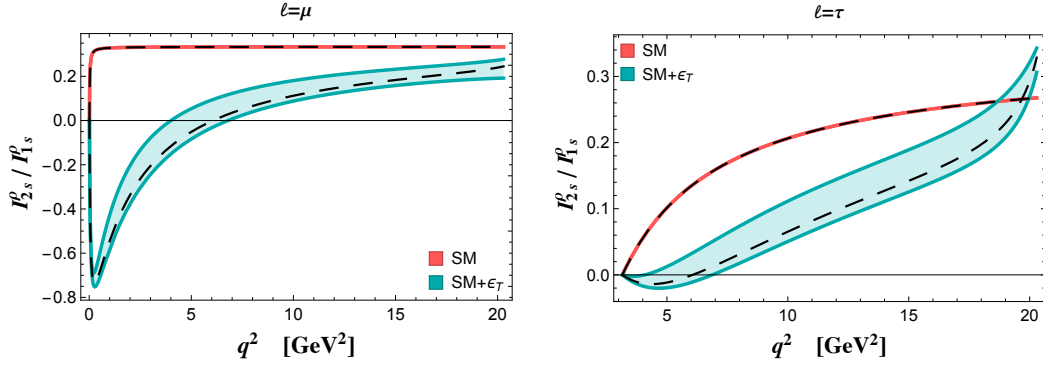


Figure 9: Ratio $R_{2s/1s}^\rho$ in (11) the modes $\bar{B} \rightarrow \rho(\pi\pi) \mu^- \bar{\nu}_\mu$ (left) and $\bar{B} \rightarrow \rho(\pi\pi) \tau^- \bar{\nu}_\tau$ (right), in SM and NP with tensor operator at the benchmark point. The dashed lines correspond to the Large Energy limit result (extrapolated to the full q^2 range).

$$(I_{6c}^\rho)|_{\epsilon_T \simeq 0} = (-8H_t^\rho H_0^\rho m_\ell) \left[m_\ell + \text{Re}[\epsilon_P] \frac{q^2}{m_b + m_u} \right], \text{ with a zero at}$$

$$q_0^2 = -\frac{m_b + m_u}{m_\ell} \frac{1}{\text{Re}[\epsilon_P]} . \quad (16)$$

This position is form factor independent, its measurement would result in a determination of $\text{Re}[\epsilon_P]$. In the left panel of Fig.11 we show I_{6c}^ρ enlarging the region where the zero is present for the benchmark $\text{Re}[\epsilon_P]$, and in the middle panel we display q_0^2 versus $\text{Re}[\epsilon_P]$ in the whole range for the coupling.

- NP with $\epsilon_P = 0$ and $\epsilon_T \neq 0$, and
 $(I_{6c}^\rho)|_{\epsilon_P \simeq 0} = (-2H_t^\rho) \left[4H_0^\rho m_\ell^2 - \text{Re}[\epsilon_T] H_L^{NP,\rho} m_\ell \sqrt{q^2} \right]$. The zero is present if $\text{Re}[\epsilon_T] > 0$. The position has a form factor dependence, as shown in Fig.11 (right panel).
- NP with both $\epsilon_P \neq 0$ and $\epsilon_T \neq 0$. In this case both real and imaginary parts of ϵ_P and ϵ_T are involved. One can notice from Fig.5 that it is possible to have two zeros, nearly coinciding with those found in the previous two cases.

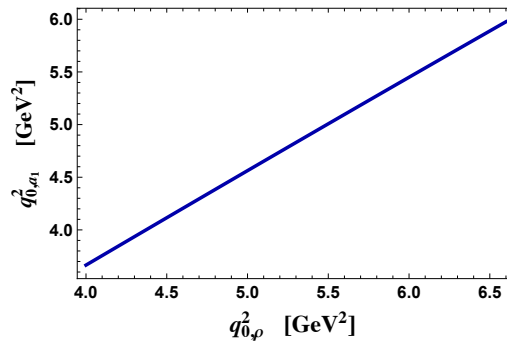


Figure 10: Relation between the position of the zeroes q_0^2 of the ratios (11) and (12) for the $B \rightarrow \rho$ and $B \rightarrow a_1$ modes, respectively.

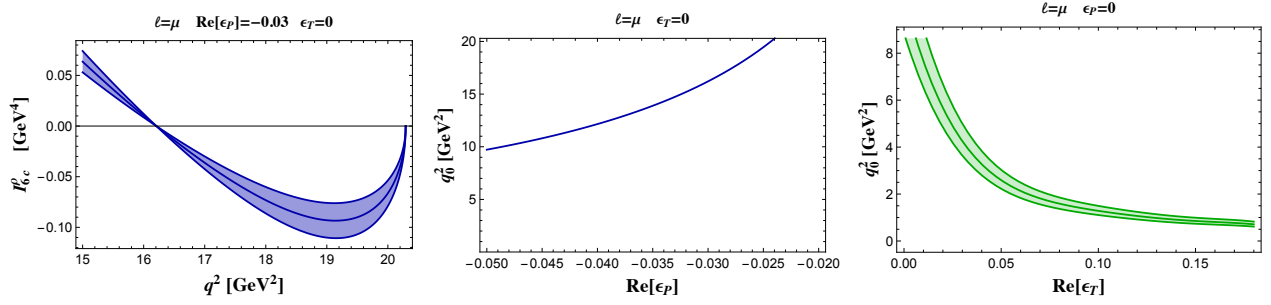


Figure 11: $\bar{B} \rightarrow \rho(\pi\pi) \mu^- \bar{\nu}_\mu$ mode: coefficient function $I_{6c}^\rho(q^2)$ (left) and position q_0^2 varying $\text{Re}(\epsilon_P)$ with $\epsilon_T = 0$ (middle panel), and $\text{Re}(\epsilon_T)$ with $\epsilon_P = 0$ (right).

Integrating the 4d differential decay distribution several observables can be constructed.

- q^2 -dependent forward-backward (FB) lepton asymmetry

$$A_{FB}(q^2) = \left[\int_0^1 d\cos\theta \frac{d^2\Gamma}{dq^2 d\cos\theta} - \int_{-1}^0 d\cos\theta \frac{d^2\Gamma}{dq^2 d\cos\theta} \right] / \frac{d\Gamma}{dq^2}, \quad (17)$$

which is given in terms of the angular coefficient functions as

$$A_{FB}(q^2) = \frac{3(I_{6c}^\rho + 2I_{6s}^\rho)}{6I_{1c}^\rho + 12I_{1s}^\rho - 2I_{2c}^\rho - 4I_{2s}^\rho}. \quad (18)$$

- Transverse forward-backward (TFB) asymmetry, the FB asymmetry for transversely polarized ρ , reading in terms of the angular coefficient functions as

$$A_{FB}^T(q^2) = \frac{3I_{6s}^\rho}{6I_{1s}^\rho - 2I_{2s}^\rho}. \quad (19)$$

For $\ell = \mu$ the asymmetries A_{FB} and A_{FB}^T are shown in Fig.12, for $\ell = \tau$ they are in Fig.14. In case of NP the zero of A_{FB} in the τ mode is shifted. Moreover, A_{FB}^T is very sensitive to the new operators, and in the case of τ it has a zero not present in SM. This is related to I_{6s}^ρ , with a zero in NP and not in SM.

- Observables sensitive to the ρ polarization. We consider the differential branching ratio for longitudinally (L) and transversely (T) polarized ρ as a function of q^2 or of one of the two angles θ , θ_V : $d\mathcal{B}_{L(T)}/dq^2$, $d\mathcal{B}_{L(T)}/d\cos\theta$ and $d\mathcal{B}_{L(T)}/d\cos\theta_V$. These observables are depicted for $\ell = \mu$ and for $\ell = \tau$ in Fig.13 and Fig.15, respectively.

Among all these quantities, the ones corresponding to transversely polarized ρ depend only on ϵ_T , as stressed in the legendae of the corresponding figures.

Integrating the distributions, we obtain in SM the longitudinal and transverse polarization fractions and the branching fractions:

$$F_L(\bar{B} \rightarrow \rho \mu^- \bar{\nu}_\mu)|_{SM} = 0.52 \pm 0.15$$

$$F_T(\bar{B} \rightarrow \rho \mu^- \bar{\nu}_\mu)|_{SM} = 0.48 \pm 0.11$$

$$\mathcal{B}(\bar{B}^0 \rightarrow \rho^+ \mu^- \bar{\nu}_\mu)|_{SM} = (3.37 \pm 0.52) \times 10^{-4} \times \left(\frac{|V_{ub}|}{0.0035} \right)^2, \quad (20)$$

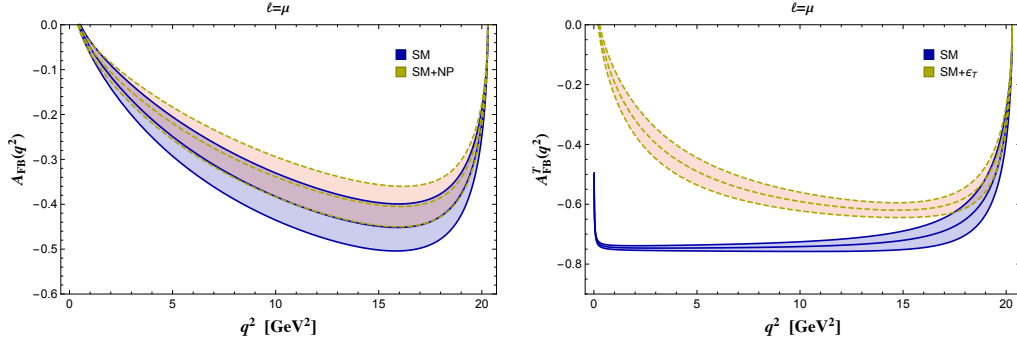


Figure 12: $\bar{B} \rightarrow \rho \mu^- \bar{\nu}_\mu$ mode: forward-backward lepton asymmetry (17) and (19) in SM and NP at the benchmark point.

$$\begin{aligned}
 F_L(\bar{B} \rightarrow \rho \tau^- \bar{\nu}_\tau)|_{SM} &= 0.50 \pm 0.13 \\
 F_T(\bar{B} \rightarrow \rho \tau^- \bar{\nu}_\tau)|_{SM} &= 0.50 \pm 0.12 \\
 \mathcal{B}(\bar{B}^0 \rightarrow \rho^+ \tau^- \bar{\nu}_\tau)|_{SM} &= (1.80 \pm 0.25) \times 10^{-4} \times \left(\frac{|V_{ub}|}{0.0035} \right)^2.
 \end{aligned} \tag{21}$$

For the $B \rightarrow \pi$ mode we have:

$$\begin{aligned}
 \mathcal{B}(\bar{B}^0 \rightarrow \pi^+ \mu^- \bar{\nu}_\mu)|_{SM} &= (1.5 \pm 0.1) \times 10^{-4} \times \left(\frac{|V_{ub}|}{0.0035} \right)^2 \\
 \mathcal{B}(\bar{B}^0 \rightarrow \pi^+ \tau^- \bar{\nu}_\tau)|_{SM} &= (0.92 \pm 0.06) \times 10^{-4} \times \left(\frac{|V_{ub}|}{0.0035} \right)^2.
 \end{aligned} \tag{22}$$

The ratios

$$R_\pi = \frac{\mathcal{B}(\bar{B} \rightarrow \pi \tau^- \bar{\nu}_\tau)}{\mathcal{B}(\bar{B} \rightarrow \pi \ell^- \bar{\nu}_\ell)}, \quad R_\rho = \frac{\mathcal{B}(\bar{B} \rightarrow \rho \tau^- \bar{\nu}_\tau)}{\mathcal{B}(\bar{B} \rightarrow \rho \ell^- \bar{\nu}_\ell)} \tag{23}$$

are modified by the New Physics operators in (1). The results in SM and NP are collected in Table 1, with the errors obtained considering the uncertainties in the hadronic form factors. The deviations are correlated when the new operators are included in the effective Hamiltonian and, as shown in Fig.16, large effects are possible in corners of the parameter space of the new effective couplings.

Concerning R_π in SM, the value $R_\pi = 0.641(17)$ is obtained using lattice form factors at large q^2 [67], the range $[0.654, 0.764]$ is found in [68], $R_\pi = 0.7$ together with $R_\rho \simeq 0.573$ is found using form factors computed in pQCD [69], $R_\pi \simeq 0.731$ and $R_\rho \simeq 0.585$ are quoted in [70]. The effect of a new charged Higgs reduces the SM result for R_π and R_ρ [71]. Considering a single NP operator per time, values for R_π up to $\simeq 4$ are obtained in [68], the range $[0.5, 1.38]$ is found in [69], while the inclusion only of the pseudoscalar and scalar operators in the effective Hamiltonian gives $R_\pi \in [0.5, 1.2]$ [49].

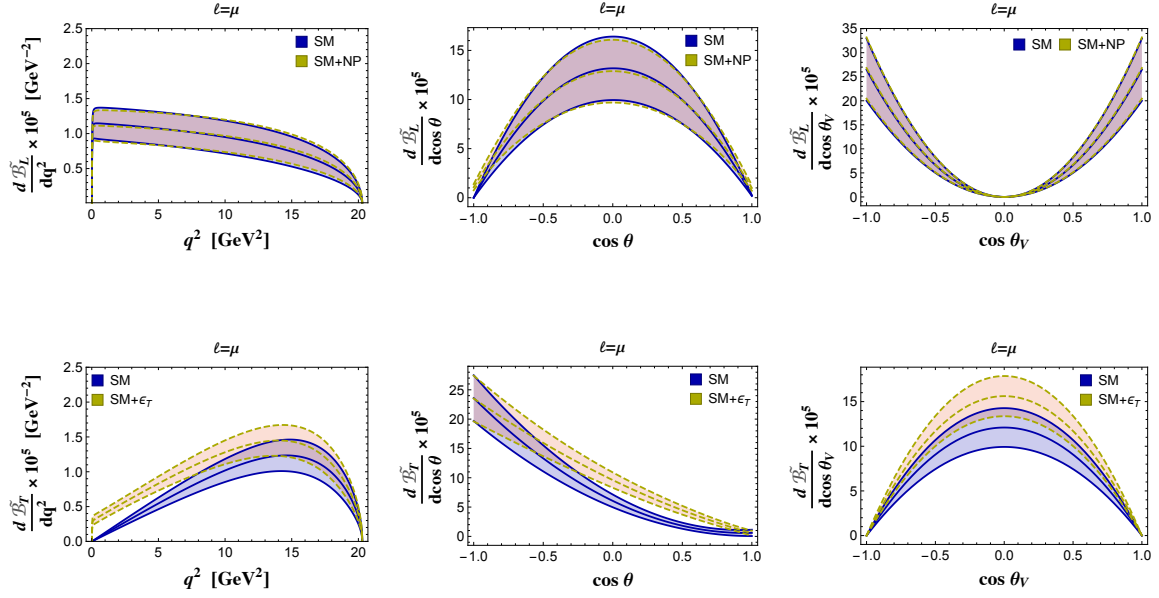


Figure 13: $\bar{B} \rightarrow \rho \mu^- \bar{\nu}_\mu$ mode: distributions $d\tilde{B}_L/dq^2$, $d\tilde{B}_L/d \cos \theta$ and $d\tilde{B}_L/d \cos \theta_V$ (first line) and $d\tilde{B}_T/dq^2$, $d\tilde{B}_T/d \cos \theta$ and $d\tilde{B}_T/d \cos \theta_V$ (second line), with $\tilde{B} = B/B(\rho \rightarrow \pi\pi)$, in SM and NP at the benchmark point.

5 Remarks about the mode $\bar{B} \rightarrow a_1(1260)\ell^-\bar{\nu}_\ell$

As for $\bar{B} \rightarrow \rho(\pi\pi)\ell^-\bar{\nu}_\ell$, the channel $\bar{B} \rightarrow a_1(\rho\pi)\ell^-\bar{\nu}_\ell$ can be numerically analyzed in SM and in the NP extension Eq.(1) using the same benchmark points for the couplings $\epsilon_{V,S,T}^\ell$, and the expressions for the angular coefficient functions in terms of the form factors. Exclusive hadronic B decays into $a_1(1260)$ have been analyzed at the B factories considering the dominant $a_1 \rightarrow \rho\pi$ mode. In particular, $B^0 \rightarrow a_1(1260)^\pm \pi^\mp$ have been scrutinized by BABAR and Belle Collaborations to carry out measurements of CP violation [72–74].

Observation and measurements of the semileptonic $\bar{B} \rightarrow a_1$ mode are within the present experimental reach, in particular at Belle II. The theoretical study of $\bar{B} \rightarrow a_1 \ell^-\bar{\nu}_\ell$ requires an assessment of the accuracy of the hadronic quantities. The $\bar{B} \rightarrow a_1$ form factors have been evaluated by different methods [75–84], but a comparative evaluation of the uncertainties has not been done so far. To present numerical examples, we use the set of form factors in Ref. [82], for which the uncertainty of about 20% is quoted. The angular coefficient functions, for the μ and τ modes and for both the ρ polarizations, are depicted in Figs.17, 18, 19 and 20.

	SM	NP (benchmark point)
R_π	0.60 ± 0.01	0.75 ± 0.02
R_ρ	0.53 ± 0.02	0.49 ± 0.02

Table 1: Ratios R_π and R_ρ in Eq.(23) in SM and in NP at the benchmark point.

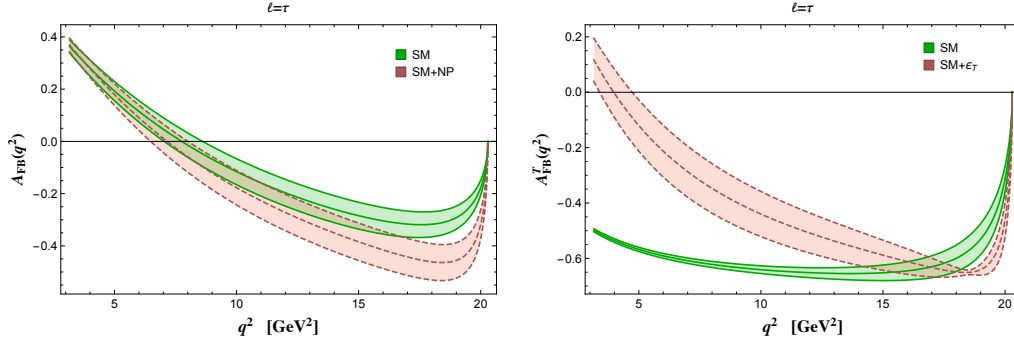


Figure 14: $\bar{B} \rightarrow \rho \tau^- \bar{\nu}_\tau$ mode: asymmetries (17) and (19) in SM and NP at the benchmark point.

In general, the hadronic uncertainties obscure the effects of the NP operators, confirming the necessity of more precise determinations. Nevertheless, there are coefficient functions in which deviations from SM can be observed, namely $I_{2s,\parallel}^{a_1}(q^2)$, $I_{6c,\parallel}^{a_1}(q^2)$ (Fig.17) and $I_{2c,\perp}^{a_1}(q^2)$ (Fig. 19) for the μ channel, $I_{1s,\parallel}^{a_1}(q^2)$, $I_{6s,\parallel}^{a_1}(q^2)$ (Fig.18) and $I_{1c,\perp}^{a_1}(q^2)$, $I_{6c,\perp}^{a_1}(q^2)$ (Fig.20) for the τ mode. On the other hand, the forward/backward lepton asymmetry shows sizeable deviations from SM in the case of τ , as shown in Fig.21.

In the ratio $R_{a_1} = \frac{\mathcal{B}(\bar{B} \rightarrow a_1 \tau^- \bar{\nu}_\tau)}{\mathcal{B}(\bar{B} \rightarrow a_1 \ell^- \bar{\nu}_\ell)}$ the form factor uncertainty is mild. We obtain, in the SM and for NP at the benchmark point,

$$R_{a_1}^{SM} = 0.44 \pm 0.07, \quad R_{a_1}^{NP} = 0.67 \pm 0.12. \quad (24)$$

The individual branching fractions in SM, in this model of form factors, are $\mathcal{B}(\bar{B} \rightarrow a_1^- \mu^- \bar{\nu}_\mu) = (3.0 \pm 1.7) \times 10^{-4}$ and $\mathcal{B}(\bar{B} \rightarrow a_1^- \tau^- \bar{\nu}_\tau) = (1.3 \pm 0.6) \times 10^{-4}$ [82].

We can now summarize the synergies between the various considered modes to provide possible evidences of NP in semileptonic $b \rightarrow u$ transitions.

- The presence of the tensor structure in the effective Hamiltonian can be established independently of the presence of the other operators, looking at deviations of the observables that depend only on ϵ_T . These are the observables involving transversely polarized ρ and a_1 . Moreover, it is possible to tightly constrain $|\epsilon_T|$ looking at the zero of the ratios defined in Eqs.(11), (12). A correlation between the position of the zero in the ρ and a_1 modes should be observed, as in Fig.10.
- If a pseudoscalar operator is present, without other NP structures, deviations should be observed in leptonic B decays and in the semileptonic decay to ρ , not in semileptonic decays to π and a_1 . Determining the position of the zero in I_{6c}^ρ allows to constrain $\text{Re}[\epsilon_P]$. Zeroes should not be present in $I_{6c,\parallel}^{a_1}$.
- If a scalar operator is present, without additional NP structures, deviations should be observed in semileptonic B decays to π and a_1 . In particular, a zero would be present in $I_{6c,\parallel}^{a_1}$, not in I_{6c}^ρ .

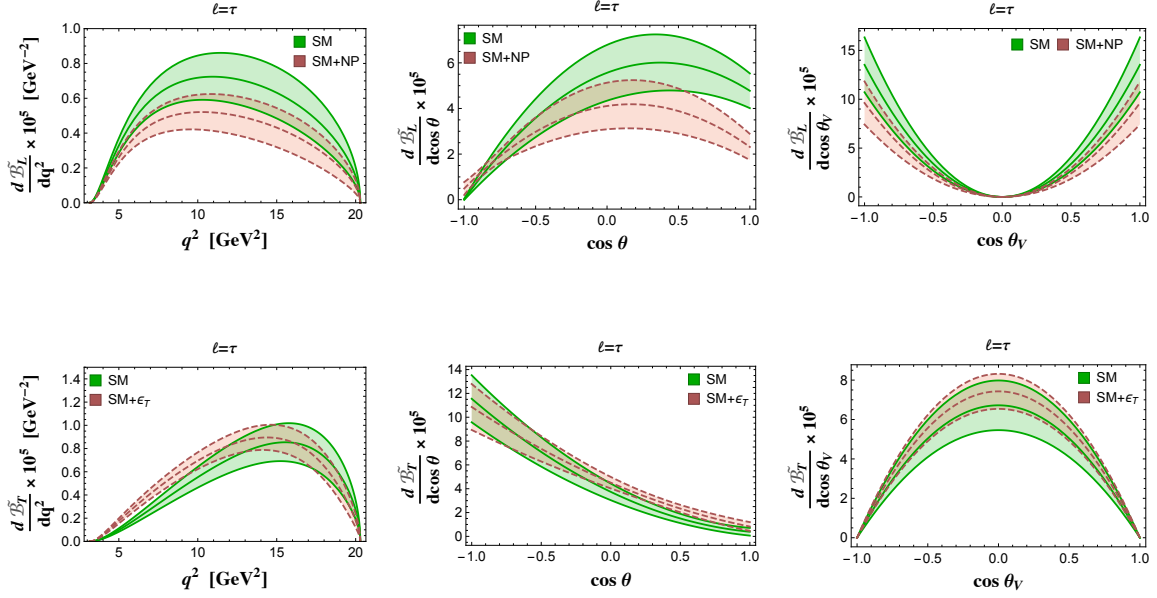


Figure 15: $\bar{B} \rightarrow \rho \tau^- \bar{\nu}_\tau$ mode: distributions $d\tilde{B}_L/dq^2$, $d\tilde{B}_L/d \cos \theta$ and $d\tilde{B}_L/d \cos \theta_V$ (first line) and $d\tilde{B}_T/dq^2$, $d\tilde{B}_T/d \cos \theta$ and $d\tilde{B}_T/d \cos \theta_V$ (second line), with $\tilde{B} = \mathcal{B}/\mathcal{B}(\rho \rightarrow \pi\pi)$, in SM and NP at the benchmark point.

- The simultaneous presence of all the operators would manifest in a more involved pattern of deviations. However, such deviations are correlated in the two modes, and the pattern of correlation can be used to assess the role of the various new terms in (1).
- Precise measurements of modes with final τ provide new important tests of LFU. The determination of R_ρ and R_π would give information on the relative sign of $\text{Re}[\epsilon_T^\mu]$ and $\text{Re}[\epsilon_T]$, as shown in Fig.16. In the a_1 channel deviations are also expected. However, in this case the reconstruction of the modes with τ is challenging: for example, using the 3 prong channel for the τ reconstruction implies to consider a final state comprising six light mesons.

6 Conclusions and perspectives

The questions arising by the anomalies in $b \rightarrow c$ semileptonic modes call for new analyses on the CKM suppressed semileptonic $b \rightarrow u$ modes, for which precise measurements are expected. We have considered an enlarged SM effective Hamiltonian including additional D=6 operators, and looked for the impact of the new terms on $\bar{B} \rightarrow \rho(\pi\pi)\ell^-\bar{\nu}_\ell$ and $\bar{B} \rightarrow a_1(\rho\pi)\ell^-\bar{\nu}_\ell$. We have constructed the 4d differential distribution for both the modes, finding that they are sensitive to different NP operators. The different quantum numbers of light mesons in the two processes act as a selection on the contributions of the NP terms, therefore the two modes provide complementary information about the role of the new operators in Eq.(1). This motivates their consideration. We have constrained the parameter space of the effective coupling constants

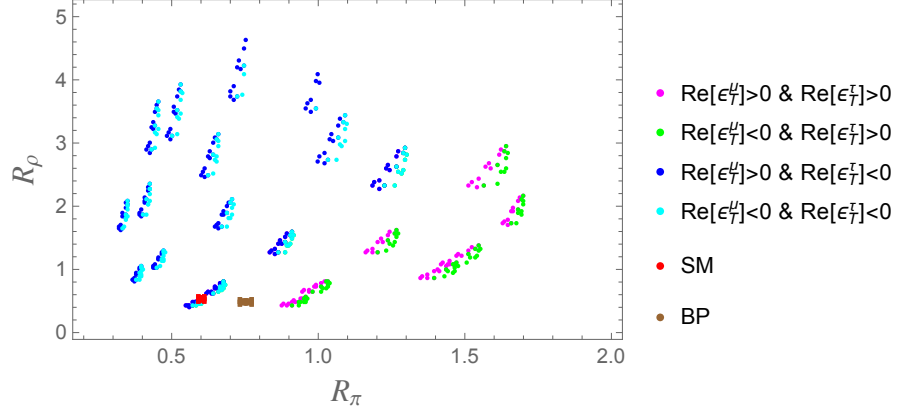


Figure 16: Correlation between R_ρ and R_π in Eq.(23) with only the tensor operator added to the SM effective Hamiltonian. The colors correspond to the different signs of $\text{Re}(\epsilon_T^\mu)$ and $\text{Re}(\epsilon_T^\tau)$ in the full range of the parameter space. The red and brown points are the SM and NP result at the benchmark point, respectively.

from current data on purely leptonic and semileptonic B modes into a pseudoscalar meson, and considered the impact on $\bar{B} \rightarrow \rho \ell^- \bar{\nu}_\ell$. Among the various observables, we have found that a few angular coefficients present zeroes that do not appear in SM, the observation of which would represent a support towards the confirmation of NP effects. We have defined integrated decay distributions, useful for comparing the modes into μ and τ , with the aim of further testing LF universality. In the perspective of precision analyses, the theoretical error connected to the hadronic matrix elements represents a sizable uncertainty needing to be reduced, in particular for the a_1 mode. The combination of different determinations based on QCD (QCD sum rules and lattice QCD), obtained in their respective domain of validity, can be a strategy for reducing the theoretical uncertainty. The Large Energy limit, in which the number of hadronic form factors is reduced, also represents a way to analyze these two modes. The possibility of finding deviations from SM fully justifies the careful scrutiny of such promising processes.

Acknowledgements. This study has been carried out within the INFN project (Iniziativa Specifica) QFT-HEP.

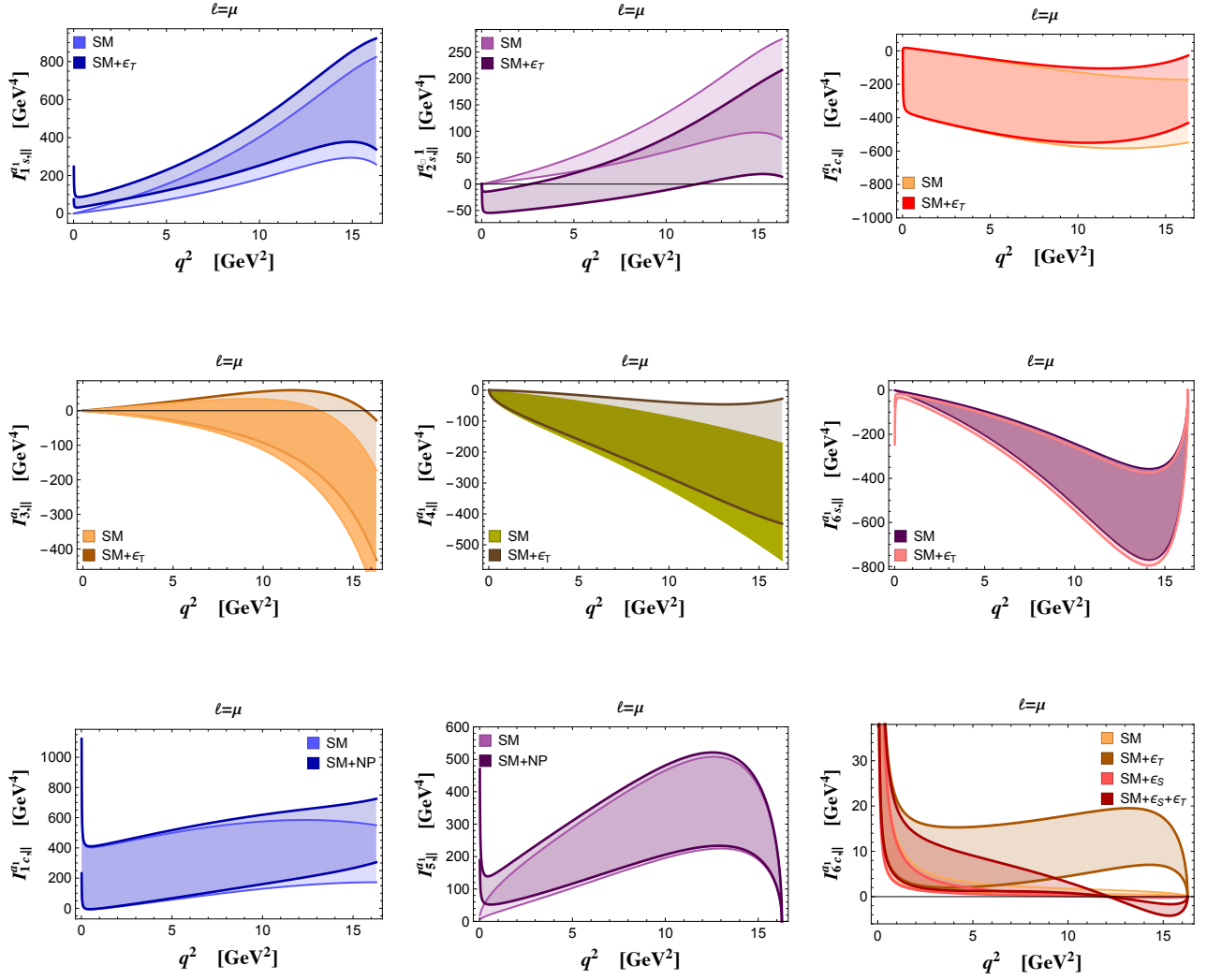


Figure 17: $\bar{B} \rightarrow a_1(\rho_{\parallel}\pi) \mu^- \bar{\nu}_{\mu}$ mode: angular coefficient functions in (8) for SM and NP at the benchmark point, using the form factors in [82]. The band widths are due to the uncertainty in the set of form factors.

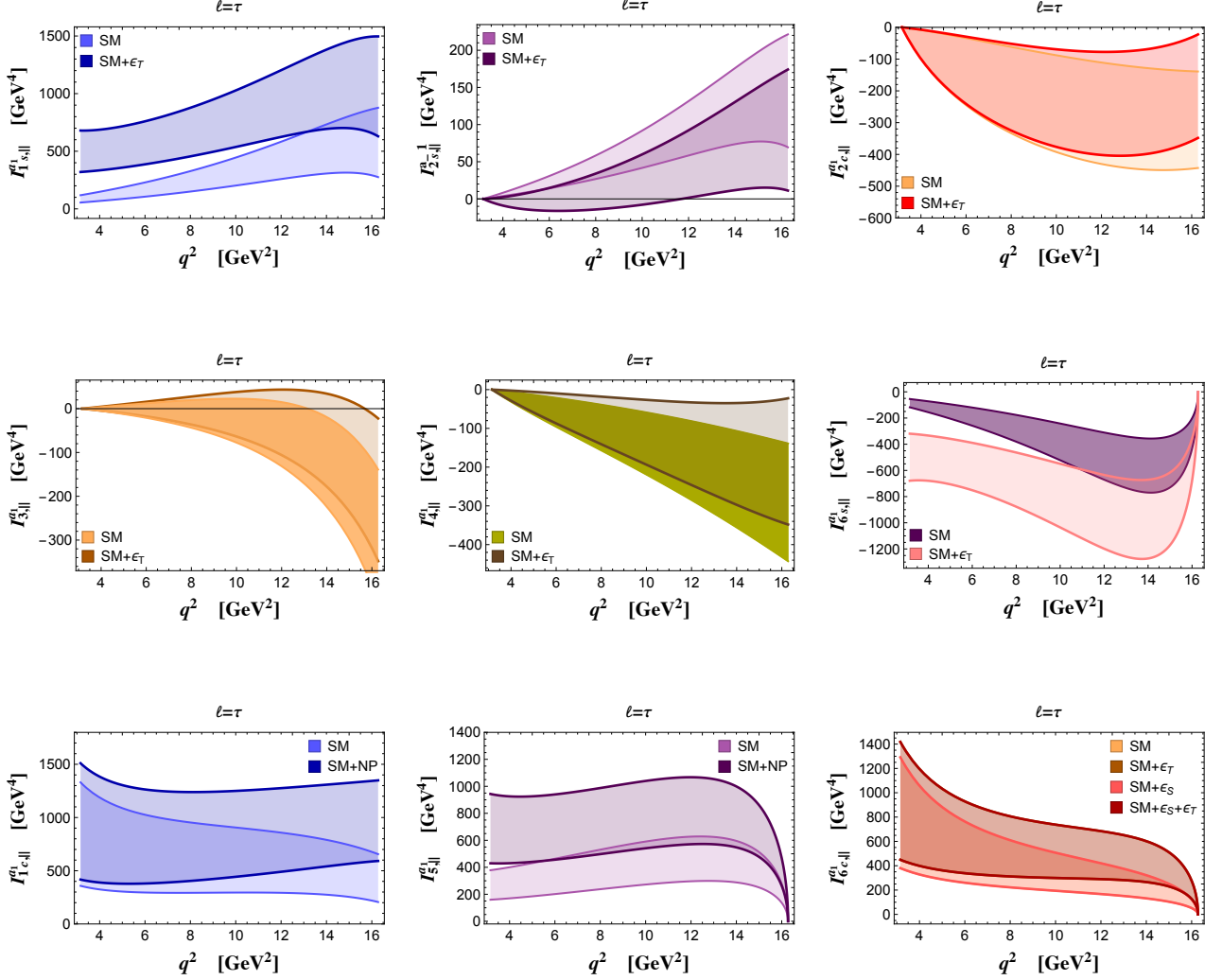


Figure 18: $\bar{B} \rightarrow a_1(\rho_{\parallel}\pi) \tau^- \bar{\nu}_\tau$ mode, angular coefficient functions with same notations as in Fig.17.

A Hadronic matrix elements

For $M_u = \pi^+$ meson, the weak matrix elements are written in terms of form factors as follows:

$$\begin{aligned}
 \langle \pi(p') | \bar{u} \gamma_\mu b | \bar{B}(p) \rangle &= f_+^{B \rightarrow \pi}(q^2) \left[p_\mu + p'_\mu - \frac{m_B^2 - m_\pi^2}{q^2} q_\mu \right] + f_0^{B \rightarrow \pi}(q^2) \frac{m_B^2 - m_\pi^2}{q^2} q_\mu \\
 \langle \pi(p') | \bar{u} b | \bar{B}(p) \rangle &= f_S^{B \rightarrow \pi}(q^2) \\
 \langle \pi(p') | \bar{u} \sigma_{\mu\nu} b | \bar{B}(p) \rangle &= -i \frac{2f_T^{B \rightarrow \pi}(q^2)}{m_B + m_\pi} [p_\mu p'_\nu - p_\nu p'_\mu] \\
 \langle \pi(p') | \bar{u} \sigma_{\mu\nu} \gamma_5 b | \bar{B}(p) \rangle &= -\frac{2f_T^{B \rightarrow \pi}(q^2)}{m_B + m_\pi} \epsilon_{\mu\nu\alpha\beta} p^\alpha p'^\beta,
 \end{aligned} \tag{A.1}$$

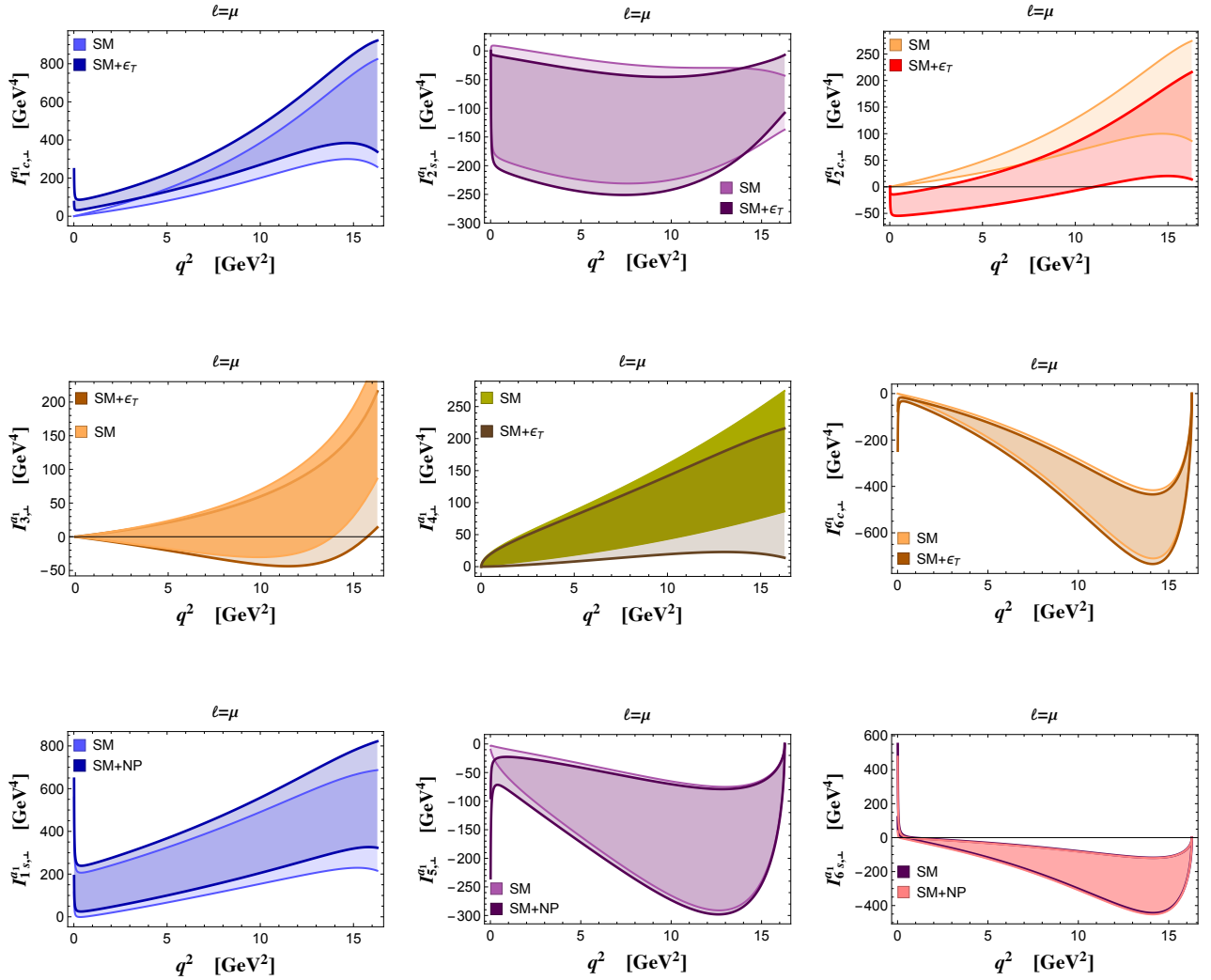


Figure 19: $\bar{B} \rightarrow a_1(\rho_\perp \pi) \mu^- \bar{\nu}_\mu$ mode, angular coefficient functions with same notations as in Fig.17.

where $\epsilon^{0123} = +1$. The relation $f_S^{B \rightarrow \pi}(q^2) = \frac{m_B^2 - m_\pi^2}{m_b - m_u} f_0^{B \rightarrow \pi}(q^2)$ holds.

For $M_u = \rho^+$ the various matrix elements, expressed in terms of form factors (with ϵ the

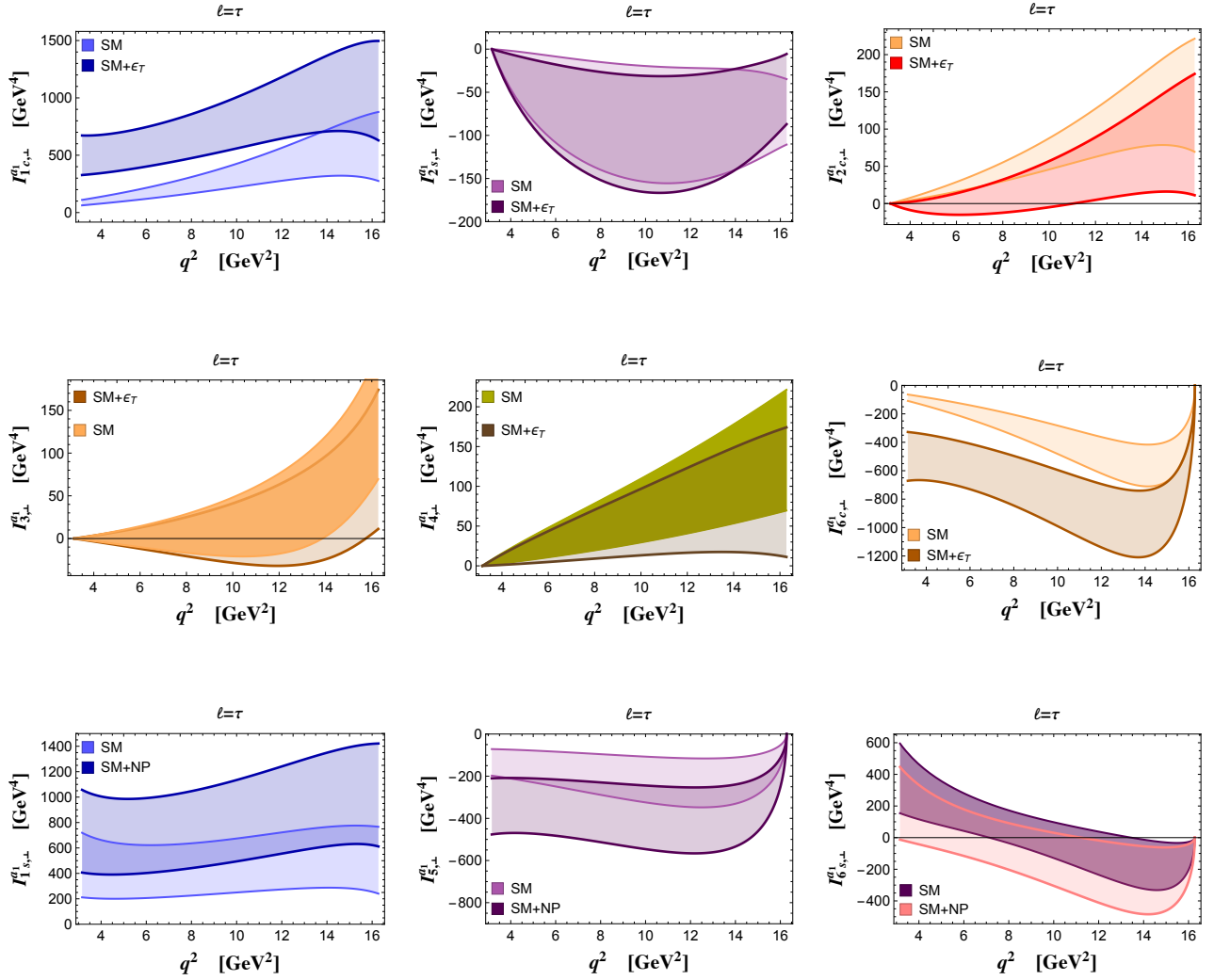


Figure 20: $\bar{B} \rightarrow a_1(\rho_\perp \pi) \tau^- \bar{\nu}_\tau$ mode, angular coefficient functions with same notations as in Fig.17.

ρ polarization vector), read:

$$\begin{aligned}
 \langle \rho(p', \epsilon) | \bar{u} \gamma_\mu (1 - \gamma_5) b | \bar{B}(p) \rangle = & -\frac{2V^{B \rightarrow \rho}(q^2)}{m_B + m_\rho} i \epsilon_{\mu\nu\alpha\beta} \epsilon^{*\nu} p^\alpha p'^\beta \\
 & - \left\{ (m_B + m_\rho) \left[\epsilon_\mu^* - \frac{(\epsilon^* \cdot q)}{q^2} q_\mu \right] A_1^{B \rightarrow \rho}(q^2) \right. \\
 & - \frac{(\epsilon^* \cdot q)}{m_B + m_\rho} \left[(p + p')_\mu - \frac{m_B^2 - m_\rho^2}{q^2} q_\mu \right] A_2^{B \rightarrow \rho}(q^2) \\
 & \left. + (\epsilon^* \cdot q) \frac{2m_\rho}{q^2} q_\mu A_0^{B \rightarrow \rho}(q^2) \right\} , \tag{A.2}
 \end{aligned}$$

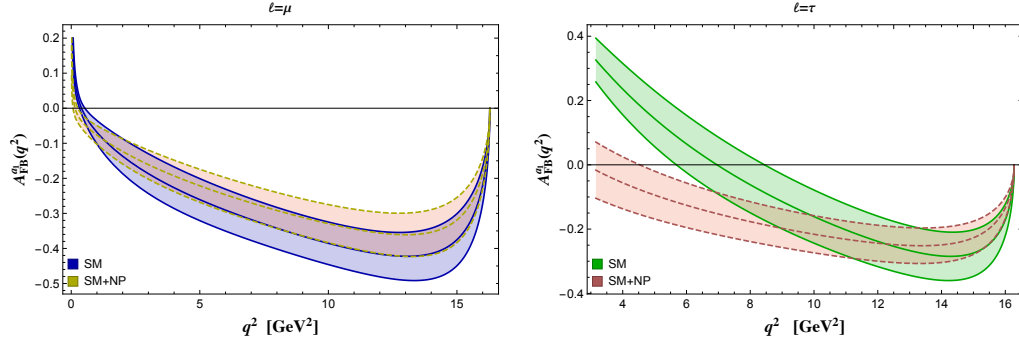


Figure 21: $\bar{B} \rightarrow a_1 \ell^- \bar{\nu}_\ell$ mode: FB lepton asymmetries for $\ell = \mu$ (left) and τ (right).

with the condition $A_0^{B \rightarrow \rho}(0) = \frac{m_B + m_\rho}{2m_\rho} A_1^{B \rightarrow \rho}(0) - \frac{m_B - m_\rho}{2m_\rho} A_2^{B \rightarrow \rho}(0)$, and

$$\langle \rho(p', \epsilon) | \bar{u} \gamma_5 b | \bar{B}(p) \rangle = -\frac{2m_\rho}{m_b + m_u} (\epsilon^* \cdot q) A_0^{B \rightarrow \rho}(q^2) \quad (\text{A.3})$$

$$\begin{aligned} \langle \rho(p', \epsilon) | \bar{u} \sigma_{\mu\nu} b | \bar{B}(p) \rangle &= T_0^{B \rightarrow \rho}(q^2) \frac{\epsilon^* \cdot q}{(m_B + m_\rho)^2} \epsilon_{\mu\nu\alpha\beta} p^\alpha p'^\beta \\ &+ T_1^{B \rightarrow \rho}(q^2) \epsilon_{\mu\nu\alpha\beta} p^\alpha \epsilon^{*\beta} + T_2^{B \rightarrow \rho}(q^2) \epsilon_{\mu\nu\alpha\beta} p'^\alpha \epsilon^{*\beta} \end{aligned} \quad (\text{A.4})$$

$$\begin{aligned} \langle \rho(p', \epsilon) | \bar{u} \sigma_{\mu\nu} \gamma_5 b | \bar{B}(p) \rangle &= i T_0^{B \rightarrow \rho}(q^2) \frac{\epsilon^* \cdot q}{(m_B + m_\rho)^2} (p_\mu p'_\nu - p_\nu p'_\mu) \\ &+ i T_1^{B \rightarrow \rho}(q^2) (p_\mu \epsilon_\nu^* - \epsilon_\mu^* p_\nu) + i T_2^{B \rightarrow \rho}(q^2) (p'_\mu \epsilon_\nu^* - \epsilon_\mu^* p'_\nu) . \end{aligned} \quad (\text{A.5})$$

For $M_u = a_1^+$ we use the decomposition:

$$\begin{aligned} \langle a_1(p', \epsilon) | \bar{u} \gamma_\mu (1 - \gamma_5) b | \bar{B}(p) \rangle &= \frac{2A^{B \rightarrow a_1}(q^2)}{m_B + m_{a_1}} i \epsilon_{\mu\nu\alpha\beta} \epsilon^{*\nu} p^\alpha p'^\beta \\ &+ \left\{ (m_B + m_{a_1}) \left[\epsilon_\mu^* - \frac{(\epsilon^* \cdot q)}{q^2} q_\mu \right] V_1^{B \rightarrow a_1}(q^2) \right. \\ &- \frac{(\epsilon^* \cdot q)}{m_B + m_{a_1}} \left[(p + p')_\mu - \frac{m_B^2 - m_{a_1}^2}{q^2} q_\mu \right] V_2^{B \rightarrow a_1}(q^2) \\ &\left. + (\epsilon^* \cdot q) \frac{2m_{a_1}}{q^2} q_\mu V_0^{B \rightarrow a_1}(q^2) \right\} \end{aligned} \quad (\text{A.6})$$

with the condition $V_0^{B \rightarrow a_1}(0) = \frac{m_B + m_{a_1}}{2m_{a_1}} V_1^{B \rightarrow a_1}(0) - \frac{m_B - m_{a_1}}{2m_{a_1}} V_2^{B \rightarrow a_1}(0)$, and

$$\langle a_1(p', \epsilon) | \bar{u}b | \bar{B}(p) \rangle = \frac{2m_{a_1}}{m_b - m_u} (\epsilon^* \cdot q) V_0^{B \rightarrow a_1}(q^2) \quad (\text{A.7})$$

$$\begin{aligned} \langle a_1(p', \epsilon) | \bar{u} \sigma_{\mu\nu} b | \bar{B}(p) \rangle &= i T_0^{B \rightarrow a_1}(q^2) \frac{\epsilon^* \cdot q}{(m_B + m_{a_1})^2} (p_\mu p'_\nu - p_\nu p'_\mu) \\ &\quad + i T_1^{B \rightarrow a_1}(q^2) (p_\mu \epsilon'_\nu - \epsilon'_\mu p_\nu) + i T_2^{B \rightarrow a_1}(q^2) (p'_\mu \epsilon'_\nu - \epsilon'_\mu p'_\nu) \end{aligned} \quad (\text{A.8})$$

$$\begin{aligned} \langle a_1(p', \epsilon) | \bar{u} \sigma_{\mu\nu} \gamma_5 b | \bar{B}(p) \rangle &= T_0^{B \rightarrow a_1}(q^2) \frac{\epsilon^* \cdot q}{(m_B + m_{a_1})^2} \epsilon_{\mu\nu\alpha\beta} p^\alpha p'^\beta \\ &\quad + T_1^{B \rightarrow a_1}(q^2) \epsilon_{\mu\nu\alpha\beta} p^\alpha \epsilon'^\beta + T_2^{B \rightarrow a_1}(q^2) \epsilon_{\mu\nu\alpha\beta} p'^\alpha \epsilon'^\beta \end{aligned} \quad (\text{A.9})$$

In the large energy (large recoil) limit for the light meson the weak matrix elements can be expressed in terms of a smaller number of form factors. We define $E = \frac{m_B^2 + m^2 - q^2}{2m_B}$ the light meson energy in the B rest-frame, and m the light meson mass. The B four-velocity is defined from $p = m_B v$, and n_- is a light-like four-vector along p' : $p' = E n_-$. In the large recoil configuration, for $E \simeq \frac{m_B}{2}$, the light quark u carries almost all the momentum of the light meson: $p'_u = E(n_-)_\mu + k_\mu$, with the residual momentum $k \ll E$. Using, e.g., a eikonal formulation of the weak current, this allows to express the form factors in terms of universal functions $\xi_i(E)$ [50, 51]. For $B \rightarrow \pi$, a single form factor $\xi_\pi(E)$ parametrizes the matrix elements,

$$\begin{aligned} \langle \pi(p') | \bar{u} \gamma_\mu b | \bar{B}(p) \rangle &= 2E \xi_\pi(E) (n_-)_\mu \\ \langle \pi(p') | \bar{u} \sigma_{\mu\nu} q^\nu b | \bar{B}(p) \rangle &= 2iE \xi_\pi(E) \left[(m_B - E)(n_-)_\mu - m_B v_\mu \right]. \end{aligned} \quad (\text{A.10})$$

For $B \rightarrow \rho$ there are two independent form factors, $\xi_\perp^\rho(E)$ and $\xi_\parallel^\rho(E)$,

$$\begin{aligned} \langle \rho(p', \epsilon) | \bar{u} \gamma_\mu b | \bar{B}(p) \rangle &= 2i E \xi_\perp^\rho(E) \epsilon_{\mu\nu\alpha\beta} \epsilon'^\nu (n_-)^\alpha v^\beta \\ \langle \rho(p', \epsilon) | \bar{u} \gamma_\mu \gamma_5 b | \bar{B}(p) \rangle &= 2E \left\{ \xi_\perp^\rho(E) [\epsilon'_\mu - (\epsilon^* \cdot v)(n_-)_\mu] + \xi_\parallel^\rho(E) (\epsilon^* \cdot v)(n_-)_\mu \right\} \\ \langle \rho(p', \epsilon) | \bar{u} \sigma_{\mu\nu} q^\nu b | \bar{B}(p) \rangle &= 2Em_B \xi_\perp^\rho(E) \epsilon_{\mu\nu\alpha\beta} \epsilon'^\nu v^\alpha (n_-)^\beta \\ \langle \rho(p', \epsilon) | \bar{u} \sigma_{\mu\nu} \gamma_5 q^\nu b | \bar{B}(p) \rangle &= -2iE \left\{ \xi_\perp^\rho(E) m_B [\epsilon'_\mu - (\epsilon^* \cdot v)(n_-)_\mu] \right. \\ &\quad \left. + \xi_\parallel^\rho(E) (\epsilon^* \cdot v) [(m_B - E)(n_-)_\mu - m_B v_\mu] \right\}, \end{aligned} \quad (\text{A.11})$$

and two independent $\xi_{\perp}^{a_1}(E)$ and $\xi_{\parallel}^{a_1}(E)$ for factors are also involved for a_1 ,

$$\begin{aligned}
\langle a_1(p', \epsilon) | \bar{u} \gamma_{\mu} \gamma_5 b | \bar{B}(p) \rangle &= -2i E \xi_{\perp}^{a_1}(E) \epsilon_{\mu\nu\alpha\beta} \epsilon^{*\nu} (n_-)^{\alpha} v^{\beta} \\
\langle a_1(p', \epsilon) | \bar{u} \gamma_{\mu} b | \bar{B}(p) \rangle &= -2E \left\{ \xi_{\perp}^{a_1}(E) [\epsilon_{\mu}^* - (\epsilon^* \cdot v)(n_-)_{\mu}] + \xi_{\parallel}^{a_1}(E) (\epsilon^* \cdot v)(n_-)_{\mu} \right\} \\
\langle a_1(p', \epsilon) | \bar{u} \sigma_{\mu\nu} q^{\nu} \gamma_5 b | \bar{B}(p) \rangle &= 2E m_B \xi_{\perp}^{a_1}(E) \epsilon_{\mu\nu\alpha\beta} \epsilon^{*\nu} v^{\alpha} (n_-)^{\beta} \\
\langle a_1(p', \epsilon) | \bar{u} \sigma_{\mu\nu} q^{\nu} b | \bar{B}(p) \rangle &= -2iE \left\{ \xi_{\perp}^{a_1}(E) m_B [\epsilon_{\mu}^* - (\epsilon^* \cdot v)(n_-)_{\mu}] \right. \\
&\quad \left. + \xi_{\parallel}^{a_1}(E) (\epsilon^* \cdot v) [(m_B - E)(n_-)_{\mu} - m_B v_{\mu}] \right\}.
\end{aligned} \tag{A.12}$$

Comparing Eqs.(A.1)-(A.8) with (A.10)-(A.12), the relations among the form factors and their large energy limit expressions can be worked out. For $B \rightarrow \pi$ they are:

$$f_+^{B \rightarrow \pi}(q^2) = \frac{m_B}{2E} f_0^{B \rightarrow \pi}(q^2) = \frac{m_B}{m_B + m_{\pi}} f_T^{B \rightarrow \pi}(q^2) = \xi_{\pi}(E), \tag{A.13}$$

for $B \rightarrow \rho$:

$$\begin{aligned}
\frac{m_B}{m_B + m_{\rho}} V^{B \rightarrow \rho}(q^2) &= \frac{m_B + m_{\rho}}{2E} A_1^{B \rightarrow \rho}(q^2) = \xi_{\perp}^{\rho}(E) \\
\frac{m_{\rho}}{E} A_0^{B \rightarrow \rho}(q^2) &= \frac{m_B + m_{\rho}}{2E} A_1^{B \rightarrow \rho}(q^2) - \frac{m_B - m_{\rho}}{m_B} A_2^{B \rightarrow \rho}(q^2) = \xi_{\parallel}^{\rho}(E) \\
T_1^{B \rightarrow \rho}(q^2) &= 0 \\
T_2^{B \rightarrow \rho}(q^2) &= 2\xi_{\perp}^{\rho}(E) \\
T_0^{B \rightarrow \rho}(q^2) &= 2\xi_{\parallel}^{\rho}(E),
\end{aligned} \tag{A.14}$$

and for $B \rightarrow a_1$:

$$\begin{aligned}
\frac{m_B}{m_B + m_{a_1}} A^{B \rightarrow a_1}(q^2) &= \frac{m_B + m_{a_1}}{2E} V_1^{B \rightarrow a_1}(q^2) = \xi_{\perp}^{a_1}(E) \\
\frac{m_{a_1}}{E} V_0^{B \rightarrow a_1}(q^2) &= \frac{m_B + m_{a_1}}{2E} V_1^{B \rightarrow a_1}(q^2) - \frac{m_B - m_{a_1}}{m_B} V_2^{B \rightarrow a_1}(q^2) = \xi_{\parallel}^{a_1}(E) \\
T_1^{B \rightarrow a_1}(q^2) &= 0 \\
T_2^{B \rightarrow a_1}(q^2) &= 2\xi_{\perp}^{a_1}(E) \\
T_0^{B \rightarrow a_1}(q^2) &= 2\xi_{\parallel}^{a_1}(E).
\end{aligned} \tag{A.15}$$

The functions ξ_{π} , ξ_{\parallel}^{ρ} and ξ_{\perp}^{ρ} have been determined by light-cone QCD sum rules within the Soft Collinear Effective Theory, using B meson light-cone distribution amplitudes [85–87].

B Angular coefficient functions

Here we collect the expressions of the angular coefficient functions in Eqs.(7,8). The general form of the $\bar{B} \rightarrow V \ell^- \bar{\nu}_\ell$ decay amplitude, with $V = \rho$ and a_1 ,

$$\mathcal{A}(\bar{B} \rightarrow V \ell^- \bar{\nu}_\ell) = \frac{G_F}{\sqrt{2}} V_{ub} \left[(1 + \epsilon_V^\ell) H_\mu^{SM} L^{SM\mu} + \epsilon_S^\ell H^{NP,S} L^{NP,S} + \epsilon_P^\ell H^{NP,P} L^{NP,P} + \epsilon_T^\ell H_{\mu\nu}^{NP,T} L^{NP,T\mu\nu} \right], \quad (\text{B.1})$$

is given in terms of the quark current matrix elements

$$H_\mu^{SM}(m) = \langle V(p_V, \epsilon(m)) | \bar{u} \gamma_\mu (1 - \gamma_5) b | \bar{B}(p_B) \rangle = \epsilon^{*\alpha}(m) T_{\mu\alpha} \quad (\text{B.2})$$

$$H^{NP,S}(m) = \langle V(p_V, \epsilon(m)) | \bar{u} b | \bar{B}(p_B) \rangle = \epsilon^{*\alpha}(m) T_\alpha^{NP,S} \quad (\text{B.3})$$

$$H_\mu^{NP,P}(m) = \langle V(p_V, \epsilon(m)) | \bar{u} \gamma_5 b | \bar{B}(p_B) \rangle = \epsilon^{*\alpha}(m) T_\alpha^{NP,P} \quad (\text{B.4})$$

$$H_{\mu\nu}^{NP,T}(m) = \langle D^*(p_{D^*}, \epsilon(m)) | \bar{c} \sigma_{\mu\nu} (1 - \gamma_5) b | \bar{B}(p_B) \rangle = \epsilon^{*\alpha}(m) T_{\mu\nu\alpha}^{NP,T} \quad (\text{B.5})$$

and of the lepton currents

$$L^{SM\mu} = \bar{\ell} \gamma^\mu (1 - \gamma_5) \nu_\ell \quad (\text{B.6})$$

$$L^{NP,S} = L^{NP,P} = \bar{\ell} (1 - \gamma_5) \nu_\ell \quad (\text{B.7})$$

$$L^{NP,T\mu\nu} = \bar{\ell} \sigma^{\mu\nu} (1 - \gamma_5) \nu_\ell. \quad (\text{B.8})$$

In SM one can relate the helicity amplitudes for the V polarization states to the polarizations of the virtual $W(q, \bar{\epsilon})$. In the lepton pair rest-frame they are:

$$\bar{\epsilon}_\pm = \frac{1}{\sqrt{2}}(0, 1, \pm i, 0) \quad , \quad \bar{\epsilon}_0 = (0, 0, 0, 1) \quad , \quad \bar{\epsilon}_t = (1, 0, 0, 0) \quad . \quad (\text{B.9})$$

This allows to define the amplitudes

$$\begin{aligned} H_m &= \bar{\epsilon}_m^{*\mu} \epsilon_m^{*\alpha} T_{\mu\alpha} & (m = 0, \pm) \\ H_t &= \bar{\epsilon}_t^{*\mu} \epsilon_0^{*\alpha} T_{\mu\alpha} & (m = t) \quad , \end{aligned} \quad (\text{B.10})$$

which can be expressed in terms of the form factors in (A.2) and (A.6):

$$\begin{aligned} H_0^\rho &= \frac{(m_B + m_\rho)^2 (m_B^2 - m_\rho^2 - q^2) A_1(q^2) - \lambda(m_B^2, m_\rho^2, q^2) A_2(q^2)}{2m_\rho(m_B + m_\rho)\sqrt{q^2}} \\ H_\pm^\rho &= \frac{(m_B + m_\rho)^2 A_1(q^2) \mp \sqrt{\lambda(m_B^2, m_\rho^2, q^2)} V(q^2)}{m_B + m_\rho} \\ H_t^\rho &= -\frac{\sqrt{\lambda(m_B^2, m_\rho^2, q^2)}}{\sqrt{q^2}} A_0(q^2) \end{aligned} \quad (\text{B.11})$$

and

$$\begin{aligned}
H_0^{a_1} &= \frac{-(m_B + m_{a_1})^2(m_B^2 - m_{a_1}^2 - q^2)V_1(q^2) + \lambda(m_B^2, m_{a_1}^2, q^2)V_2(q^2)}{2m_{a_1}(m_B + m_{a_1})\sqrt{q^2}} \\
H_{\pm}^{a_1} &= \frac{-(m_B + m_{a_1})^2V_1(q^2) \pm \sqrt{\lambda(m_B^2, m_{a_1}^2, q^2)}A(q^2)}{m_B + m_{a_1}} \\
H_t^{a_1} &= \frac{\sqrt{\lambda(m_B^2, m_{a_1}^2, q^2)}}{\sqrt{q^2}} V_0(q^2) .
\end{aligned} \tag{B.12}$$

No new definitions are needed in the case of S and P operators, since their matrix elements involve the same form factors as in SM. For the NP tensor operator one defines [32]:

$$\begin{aligned}
H_+^{NP, \rho} &= \frac{1}{\sqrt{q^2}} \left\{ [m_B^2 - m_\rho^2 + \lambda^{1/2}(m_B^2, m_\rho^2, q^2)] (T_1^{B \rightarrow \rho} + T_2^{B \rightarrow \rho}) + q^2(T_1^{B \rightarrow \rho} - T_2^{B \rightarrow \rho}) \right\} \\
H_-^{NP, \rho} &= \frac{1}{\sqrt{q^2}} \left\{ [m_B^2 - m_\rho^2 - \lambda^{1/2}(m_B^2, m_\rho^2, q^2)] (T_1^{B \rightarrow \rho} + T_2^{B \rightarrow \rho}) + q^2(T_1^{B \rightarrow \rho} - T_2^{B \rightarrow \rho}) \right\} \\
H_L^{NP, \rho} &= 4 \left\{ \frac{\lambda(m_B^2, m_\rho^2, q^2)}{m_\rho(m_B + m_\rho)^2} T_0^{B \rightarrow \rho} + 2 \frac{m_B^2 + m_\rho^2 - q^2}{m_\rho} T_1^{B \rightarrow \rho} + 4m_\rho T_2^{B \rightarrow \rho} \right\} .
\end{aligned} \tag{B.13}$$

The expressions for $H_{(+,-,L)}^{NP, a_1}$ are obtained replacing $m_\rho \rightarrow m_{a_1}$ and $T_i^{B \rightarrow \rho} \rightarrow T_i^{B \rightarrow a_1}$.

For the decay $\bar{B} \rightarrow a_1(\rho\pi)\ell^-\bar{\nu}_\ell$ we define the ρ helicity amplitudes $\mathcal{A}_1, \mathcal{A}_{-1}, \mathcal{A}_0$ for $\lambda = +1, -1, 0$. Writing the matrix element

$$\langle \rho(p_\rho, \eta) \pi(p_\pi) | a_1(p', \epsilon) \rangle = g_1 (\epsilon \cdot \eta^*) (p' \cdot p_\rho) + g_2 (\epsilon \cdot p_\rho) (p' \cdot \eta^*) \tag{B.14}$$

in terms of the couplings g_1 and g_2 , we have:

$$\Gamma(a_1 \rightarrow \rho\pi) = \frac{|\vec{p}_\rho|}{24\pi m_{a_1}^2} \left(\tilde{\Gamma}_\perp + \tilde{\Gamma}_\parallel \right), \tag{B.15}$$

where $|\vec{p}_\rho| = \frac{\lambda^{1/2}(m_{a_1}^2, m_\rho^2, m_\pi^2)}{2m_{a_1}}$ and

$$\begin{aligned}
\tilde{\Gamma}_\perp &= 2|\mathcal{A}_1|^2 = 2g_1^2 m_{a_1}^2 (m_\rho^2 + |\vec{p}_\rho|^2) \\
\tilde{\Gamma}_\parallel &= |\mathcal{A}_0|^2 = \frac{m_{a_1}^2}{m_\rho^2} \left[(m_\rho^2 + |\vec{p}_\rho|^2) g_1 + |\vec{p}_\rho|^2 g_2 \right]^2 .
\end{aligned} \tag{B.16}$$

The branching ratios for ρ longitudinally and transversely polarized, appearing in the factors $\mathcal{N}_{a_1}^{||(\perp)}$ in Eq.(8), read:

$$\mathcal{B}(a_1 \rightarrow \rho_{||(\perp)} \pi) = \frac{1}{\Gamma(a_1)} \frac{|\vec{p}_\rho|}{24\pi m_{a_1}^2} \tilde{\Gamma}_{||(\perp)}. \tag{B.17}$$

Table 2: Angular coefficient functions in the 4d $\bar{B} \rightarrow \rho(\pi\pi)\ell^-\bar{\nu}_\ell$ decay distribution, Eq.(7), in SM.

i	I_i^{SM}
I_{1s}^ρ	$\frac{1}{2}(H_+^2 + H_-^2)(m_\ell^2 + 3q^2)$
I_{1c}^ρ	$4m_\ell^2 H_t^2 + 2H_0^2(m_\ell^2 + q^2)$
I_{2s}^ρ	$-\frac{1}{2}(H_+^2 + H_-^2)(m_\ell^2 - q^2)$
I_{2c}^ρ	$2H_0^2(m_\ell^2 - q^2)$
I_3^ρ	$2H_+H_-(m_\ell^2 - q^2)$
I_4^ρ	$H_0(H_+ + H_-)(m_\ell^2 - q^2)$
I_5^ρ	$-2H_t(H_+ + H_-)m_\ell^2 - 2H_0(H_+ - H_-)q^2$
I_{6s}^ρ	$2(H_+^2 - H_-^2)q^2$
I_{6c}^ρ	$-8H_tH_0m_\ell^2$
I_7^ρ	0

C $B \rightarrow \pi$ form factors and other parameters

For the $B \rightarrow \pi$ form factors defined in (A.1) we use the parametrization [88]

$$f_{+,T}(t) = \frac{1}{1 - \frac{q^2}{m_{pole}^2}} \sum_{n=0}^{N-1} a_n \left[z(t)^n - \frac{n}{N} (-1)^{n-N} z(t)^N \right]$$

$$f_0(t) = \sum_{n=0}^{N-1} a_n z(t)^n, \quad (\text{C.1})$$

expressed as a truncated series in the variable

$$z(t) = \frac{\sqrt{t_+ - t} - \sqrt{t_+ - t_0}}{\sqrt{t_+ - t} + \sqrt{t_+ - t_0}}. \quad (\text{C.2})$$

In this expression $t_+ = (m_B + m_\pi)^2$, and t_0 is chosen at the value $t_0 = (m_B + m_\pi) (\sqrt{m_B} - \sqrt{m_\pi})^2$. For $\bar{B} \rightarrow \pi\mu^-\bar{\nu}_\mu$ the kinematic range is $-0.279 \leq z \leq 0.283$, for $\bar{B} \rightarrow \pi\tau^-\bar{\nu}_\tau$ it is $-0.279 \leq z \leq 0.257$. The mass of the pole in $f_{+,T}$ is $m_{pole} = m_{B^*}$. The parameters a_n for f_+ , f_0 and f_T , with the condition $f_+(0) = f_0(0)$, are obtained fitting the Light-Cone QCD sum rule results in the range $m_c^2 \leq q^2 \leq 12 \text{ GeV}^2$ [62, 63] and the lattice QCD results for $16 \text{ GeV}^2 \leq q^2$ in the recent FLAG report [64]: they are in Table 10. The other parameters used in the analysis are the quark masses $m_u = 2.16_{-0.26}^{+0.49} \text{ MeV}$ (in the \overline{MS} scheme at $\mu = 2 \text{ GeV}$), $\bar{m}_b(\bar{m}_b) = 4.18_{-0.03}^{+0.04} \text{ GeV}$ [59], and the B decay constant $f_B = 188 \pm 7 \text{ MeV}$ [64].

Table 3: Angular coefficient functions for $\bar{B} \rightarrow \rho(\pi\pi)\ell^-\bar{\nu}_\ell$: NP term with P operator, interference term SM-NP with P operator, and NP-NP interference terms between P and T operators, Eq.(9).

i	$I_i^{\text{NP},P}$	$I_i^{\text{INT},P}$	$I_i^{\text{INT},PT}$
I_{1s}^ρ	0	0	0
I_{1c}^ρ	$4H_t^2 \frac{q^4}{(m_b+m_u)^2}$	$4H_t^2 \frac{m_\ell q^2}{m_b+m_u}$	0
I_{2s}^ρ	0	0	0
I_{2c}^ρ	0	0	0
I_3^ρ	0	0	0
I_4^ρ	0	0	0
I_5^ρ	0	$-H_t(H_+ + H_-) \frac{m_\ell q^2}{m_b+m_u}$	$2H_t(H_+^{\text{NP}} + H_-^{\text{NP}}) \frac{(q^2)^{3/2}}{m_b+m_u}$
I_{6s}^ρ	0	0	0
I_{6c}^ρ	0	$-4H_t H_0 \frac{m_\ell q^2}{m_b+m_u}$	$H_t H_L^{\text{NP}} \frac{(q^2)^{3/2}}{m_b+m_u}$
I_7^ρ	0	$-H_t(H_+ - H_-) \frac{m_\ell q^2}{m_b+m_u}$	$2H_t(H_+^{\text{NP}} - H_-^{\text{NP}}) \frac{(q^2)^{3/2}}{m_b+m_u}$

Table 4: Angular coefficient functions for $\bar{B} \rightarrow \rho(\pi\pi)\ell^-\bar{\nu}_\ell$: NP term with T operator and interference term SM-NP with T operator, Eq.(9).

i	$I_i^{\text{NP},T}$	$I_i^{\text{INT},T}$
I_{1s}^ρ	$2[(H_+^{\text{NP}})^2 + (H_-^{\text{NP}})^2](3m_\ell^2 + q^2)$	$-4(H_+^{\text{NP}} H_+ + H_-^{\text{NP}} H_-) m_\ell \sqrt{q^2}$
I_{1c}^ρ	$\frac{1}{8}(H_L^{\text{NP}})^2(m_\ell^2 + q^2)$	$-H_L^{\text{NP}} H_0 m_\ell \sqrt{q^2}$
I_{2s}^ρ	$2[(H_+^{\text{NP}})^2 + (H_-^{\text{NP}})^2](m_\ell^2 - q^2)$	0
I_{2c}^ρ	$\frac{1}{8}(H_L^{\text{NP}})^2(q^2 - m_\ell^2)$	0
I_3^ρ	$8H_+^{\text{NP}} H_-^{\text{NP}}(q^2 - m_\ell^2)$	0
I_4^ρ	$\frac{1}{2}H_L^{\text{NP}}(H_+^{\text{NP}} + H_-^{\text{NP}})(q^2 - m_\ell^2)$	0
I_5^ρ	$-H_L^{\text{NP}}(H_+^{\text{NP}} - H_-^{\text{NP}})m_\ell^2$	$\frac{1}{4}[H_L^{\text{NP}}(H_+ - H_-) + 8H_+^{\text{NP}}(H_t + H_0) + 8H_-^{\text{NP}}(H_t - H_0)]m_\ell \sqrt{q^2}$
I_{6s}^ρ	$8[(H_+^{\text{NP}})^2 - (H_-^{\text{NP}})^2]m_\ell^2$	$-4(H_+^{\text{NP}} H_+ - H_-^{\text{NP}} H_-)m_\ell \sqrt{q^2}$
I_{6c}^ρ	0	$H_L^{\text{NP}} H_t m_\ell \sqrt{q^2}$
I_7^ρ	0	$\frac{1}{4}[H_L^{\text{NP}}(H_+ + H_-) - 8H_+^{\text{NP}}(H_t + H_0) + 8H_-^{\text{NP}}(H_t - H_0)]m_\ell \sqrt{q^2}$

Table 5: Angular coefficient functions in the 4d $\bar{B} \rightarrow a_1(\rho\pi)\ell^-\bar{\nu}_\ell$ decay distribution, Eq.(8), in SM.

i	$I_{i,\parallel}^{\text{SM}}$	$I_{i,\perp}^{\text{SM}}$
$I_{1s}^{a_1}$	$\frac{1}{2}(H_+^2 + H_-^2)(m_\ell^2 + 3q^2)$	$2H_t^2 m_\ell^2 + H_0^2(m_\ell^2 + q^2) + \frac{1}{4}(H_+^2 + H_-^2)(m_\ell^2 + 3q^2)$
$I_{1c}^{a_1}$	$4H_t^2 m_\ell^2 + 2H_0^2(m_\ell^2 + q^2)$	$\frac{1}{2}(H_+^2 + H_-^2)(m_\ell^2 + 3q^2)$
$I_{2s}^{a_1}$	$-\frac{1}{2}(H_+^2 + H_-^2)(m_\ell^2 - q^2)$	$[H_0^2 - \frac{1}{4}(H_+^2 + H_-^2)](m_\ell^2 - q^2)$
$I_{2c}^{a_1}$	$2H_0^2(m_\ell^2 - q^2)$	$-\frac{1}{2}(H_+^2 + H_-^2)(m_\ell^2 - q^2)$
$I_3^{a_1}$	$2H_+ H_- (m_\ell^2 - q^2)$	$-H_+ H_- (m_\ell^2 - q^2)$
$I_4^{a_1}$	$H_0(H_+ + H_-)(m_\ell^2 - q^2)$	$-\frac{1}{2}H_0(H_+ + H_-)(m_\ell^2 - q^2)$
$I_5^{a_1}$	$-2H_t(H_+ + H_-)m_\ell^2 - 2H_0(H_+ - H_-)q^2$	$H_t(H_+ + H_-)m_\ell^2 + H_0(H_+ - H_-)q^2$
$I_{6s}^{a_1}$	$2(H_+^2 - H_-^2)q^2$	$-4H_t H_0 m_\ell^2 + (H_+^2 - H_-^2)q^2$
$I_{6c}^{a_1}$	$-8H_t H_0 m_\ell^2$	$2(H_+^2 - H_-^2)q^2$
$I_7^{a_1}$	0	0

Table 6: Angular coefficient functions for $\bar{B} \rightarrow a_1(\rho\pi)\ell^-\bar{\nu}_\ell$: NP term with S operator, interference SM-NP with S operator, and NP-NP interference with S and T operators, Eq.(9).

i	$I_{i,\parallel}^{\text{NP},S}$	$I_{i,\parallel}^{\text{INT},S}$	$I_{i,\parallel}^{\text{INT},ST}$
$I_{1s}^{a_1}$	0	0	0
$I_{1c}^{a_1}$	$4H_t^2 \frac{q^4}{(m_b - m_u)^2}$	$4H_t^2 \frac{m_\ell q^2}{m_b - m_u}$	0
$I_{2s}^{a_1}$	0	0	0
$I_{2c}^{a_1}$	0	0	0
$I_3^{a_1}$	0	0	0
$I_4^{a_1}$	0	0	0
$I_5^{a_1}$	0	$-H_t(H_+ + H_-) \frac{m_\ell q^2}{m_b - m_u}$	$-2H_t(H_+^{NP} + H_-^{NP}) \frac{(q^2)^{3/2}}{m_b - m_u}$
$I_{6s}^{a_1}$	0	0	0
$I_{6c}^{a_1}$	0	$-4H_t H_0 \frac{m_\ell q^2}{m_b - m_u}$	$-H_t H_L^{NP} \frac{(q^2)^{3/2}}{m_b - m_u}$
$I_7^{a_1}$	0	$-H_t(H_+ - H_-) \frac{m_\ell q^2}{m_b - m_u}$	$-2H_t(H_+^{NP} - H_-^{NP}) \frac{(q^2)^{3/2}}{m_b - m_u}$

Table 7: Angular coefficient functions for $\bar{B} \rightarrow a_1(\rho\pi)\ell^-\bar{\nu}_\ell$: NP term with S operator, interference SM-NP with S operator, and NP-NP interference with S and T operators, Eq.(9).

i	$I_{i,\perp}^{\text{NP},S}$	$I_{i,\perp}^{\text{INT},S}$	$I_{i,\perp}^{\text{INT},ST}$
$I_{1s}^{a_1}$	$2H_t^2 \frac{q^4}{(m_b-m_u)^2}$	$2H_t^2 \frac{m_\ell q^2}{m_b-m_u}$	0
$I_{1c}^{a_1}$	0	0	0
$I_{2s}^{a_1}$	0	0	0
$I_{2c}^{a_1}$	0	0	0
$I_3^{a_1}$	0	0	0
$I_4^{a_1}$	0	0	0
$I_5^{a_1}$	0	$\frac{1}{2}H_t(H_+ + H_-)\frac{m_\ell q^2}{m_b-m_u}$	$H_t(H_+^{\text{NP}} + H_-^{\text{NP}})\frac{(q^2)^{3/2}}{m_b-m_u}$
$I_{6s}^{a_1}$	0	$-2H_t H_0 \frac{m_\ell q^2}{m_b-m_u}$	$-H_t H_L^{\text{NP}} \frac{(q^2)^{3/2}}{2(m_b-m_u)}$
$I_{6c}^{a_1}$	0	0	0
$I_7^{a_1}$	0	$\frac{1}{2}H_t(H_+ - H_-)\frac{m_\ell q^2}{m_b-m_u}$	$H_t(H_+^{\text{NP}} - H_-^{\text{NP}})\frac{(q^2)^{3/2}}{m_b-m_u}$

Table 8: Angular coefficient functions for $\bar{B} \rightarrow a_1(\rho\pi)\ell^-\bar{\nu}_\ell$: NP term with T operator and interference SM-NP with T operator.

i	$I_{i,\parallel}^{\text{NP},T}$	$I_{i,\parallel}^{\text{INT},T}$
$I_{1s}^{a_1}$	$2[(H_+^{\text{NP}})^2 + (H_-^{\text{NP}})^2](3m_\ell^2 + q^2)$	$4(H_+^{\text{NP}} H_+ + H_-^{\text{NP}} H_-)m_\ell \sqrt{q^2}$
$I_{1c}^{a_1}$	$\frac{1}{8}(H_L^{\text{NP}})^2(m_\ell^2 + q^2)$	$H_L^{\text{NP}} H_0 m_\ell \sqrt{q^2}$
$I_{2s}^{a_1}$	$2[(H_+^{\text{NP}})^2 + (H_-^{\text{NP}})^2](m_\ell^2 - q^2)$	0
$I_{2c}^{a_1}$	$-\frac{1}{8}(H_L^{\text{NP}})^2(m_\ell^2 - q^2)$	0
$I_3^{a_1}$	$-8H_+^{\text{NP}} H_-^{\text{NP}}(m_\ell^2 - q^2)$	0
$I_4^{a_1}$	$-\frac{1}{2}H_L^{\text{NP}}(H_+^{\text{NP}} + H_-^{\text{NP}})(m_\ell^2 - q^2)$	0
$I_5^{a_1}$	$-H_L^{\text{NP}}(H_+^{\text{NP}} - H_-^{\text{NP}})m_\ell^2$	$-\frac{1}{4}[H_L^{\text{NP}}(H_+ - H_-) + 8H_+^{\text{NP}}(H_t + H_0) + 8H_-^{\text{NP}}(H_t - H_0)]m_\ell \sqrt{q^2}$
$I_{6s}^{a_1}$	$8[(H_+^{\text{NP}})^2 - (H_-^{\text{NP}})^2]m_\ell^2$	$4(H_+^{\text{NP}} H_+ - H_-^{\text{NP}} H_-)m_\ell \sqrt{q^2}$
$I_{6c}^{a_1}$	0	$-H_L^{\text{NP}} H_t m_\ell \sqrt{q^2}$
$I_7^{a_1}$	0	$-\frac{1}{4}[H_L^{\text{NP}}(H_+ + H_-) - 8H_+^{\text{NP}}(H_t + H_0) + 8H_-^{\text{NP}}(H_t - H_0)]m_\ell \sqrt{q^2}$

Table 9: Angular coefficient functions for $\bar{B} \rightarrow a_1(\rho\pi)\ell^-\bar{\nu}_\ell$: NP term with T operator and interference SM-NP with T operator, Eq.(9).

i	$I_{i,\perp}^{\text{NP},T}$	$I_{i,\perp}^{\text{INT},T}$
$I_{1s}^{a_1}$	$[(H_+^{\text{NP}})^2 + (H_-^{\text{NP}})^2](3m_\ell^2 + q^2)$ $+ \frac{1}{16}(H_L^{\text{NP}})^2(m_\ell^2 + q^2)$	$\frac{1}{2}[4(H_+^{\text{NP}}H_+ + H_-^{\text{NP}}H_-)$ $+ H_L^{\text{NP}}H_0]m_\ell\sqrt{q^2}$
$I_{1c}^{a_1}$	$2[(H_+^{\text{NP}})^2 + (H_-^{\text{NP}})^2](3m_\ell^2 + q^2)$	$4(H_+^{\text{NP}}H_+ + H_-^{\text{NP}}H_-)m_\ell\sqrt{q^2}$
$I_{2s}^{a_1}$	$[(H_+^{\text{NP}})^2 + (H_-^{\text{NP}})^2](m_\ell^2 - q^2)$ $- \frac{1}{16}(H_L^{\text{NP}})^2(m_\ell^2 - q^2)$	0
$I_{2c}^{a_1}$	$2[(H_+^{\text{NP}})^2 + (H_-^{\text{NP}})^2](m_\ell^2 - q^2)$	0
$I_3^{a_1}$	$4H_+^{\text{NP}}H_-^{\text{NP}}(m_\ell^2 - q^2)$	0
$I_4^{a_1}$	$\frac{1}{4}H_L^{\text{NP}}(H_+^{\text{NP}} + H_-^{\text{NP}})(m_\ell^2 - q^2)$	0
$I_5^{a_1}$	$\frac{1}{2}H_L^{\text{NP}}(H_+^{\text{NP}} - H_-^{\text{NP}})m_\ell^2$	$\frac{1}{8}[H_L^{\text{NP}}(H_+ - H_-) + 8H_+^{\text{NP}}(H_t + H_0)$ $+ 8H_-^{\text{NP}}(H_t - H_0)]m_\ell\sqrt{q^2}$
$I_{6s}^{a_1}$	$4[(H_+^{\text{NP}})^2 - (H_-^{\text{NP}})^2]m_\ell^2$	$-\frac{1}{2}[-4(H_+^{\text{NP}}H_+ - H_-^{\text{NP}}H_-) + H_L^{\text{NP}}H_t]m_\ell\sqrt{q^2}$
$I_{6c}^{a_1}$	$8[(H_+^{\text{NP}})^2 - (H_-^{\text{NP}})^2]m_\ell^2$	$4(H_+^{\text{NP}}H_+ - H_-^{\text{NP}}H_-)m_\ell\sqrt{q^2}$
$I_7^{a_1}$	0	$\frac{1}{8}[H_L^{\text{NP}}(H_+ + H_-) - 8H_+^{\text{NP}}(H_t + H_0)$ $+ 8H_-^{\text{NP}}(H_t - H_0)]$

Table 10: $B \rightarrow \pi$ form factor parameters in Eq.(C.1).

	$f_+^{B \rightarrow \pi}$	$f_0^{B \rightarrow \pi}$	$f_T^{B \rightarrow \pi}$
a_0	0.416 (20)	0.492 (20)	0.400 (21)
a_1	-0.430	-1.35	-0.50
a_2	0.114	2.50	0.00076
a_3			0.534

References

- [1] **BaBar** Collaboration, J. P. Lees et al., *Evidence for an excess of $\bar{B} \rightarrow D^{(*)}\tau^-\bar{\nu}_\tau$ decays*, *Phys. Rev. Lett.* **109** (2012) 101802, [[arXiv:1205.5442](#)].
- [2] **BaBar** Collaboration, J. P. Lees et al., *Measurement of an Excess of $\bar{B} \rightarrow D^{(*)}\tau^-\bar{\nu}_\tau$ Decays and Implications for Charged Higgs Bosons*, *Phys. Rev.* **D88** (2013) 072012, [[arXiv:1303.0571](#)].
- [3] **Belle** Collaboration, M. Huschle et al., *Measurement of the branching ratio of $\bar{B} \rightarrow D^{(*)}\tau^-\bar{\nu}_\tau$ relative to $\bar{B} \rightarrow D^{(*)}\ell^-\bar{\nu}_\ell$ decays with hadronic tagging at Belle*, *Phys. Rev.* **D92** (2015) 072014, [[arXiv:1507.03233](#)].
- [4] **Belle** Collaboration, Y. Sato et al., *Measurement of the branching ratio of $\bar{B}^0 \rightarrow D^{*+}\tau^-\bar{\nu}_\tau$ relative to $\bar{B}^0 \rightarrow D^{*+}\ell^-\bar{\nu}_\ell$ decays with a semileptonic tagging method*, *Phys. Rev.* **D94** (2016) 072007, [[arXiv:1607.07923](#)].
- [5] **Belle** Collaboration, S. Hirose et al., *Measurement of the τ lepton polarization and $R(D^*)$ in the decay $\bar{B} \rightarrow D^*\tau^-\bar{\nu}_\tau$* , *Phys. Rev. Lett.* **118** (2017) 211801, [[arXiv:1612.00529](#)].
- [6] **Belle** Collaboration, S. Hirose et al., *Measurement of the τ lepton polarization and $R(D^*)$ in the decay $\bar{B} \rightarrow D^*\tau^-\bar{\nu}_\tau$ with one-prong hadronic τ decays at Belle*, *Phys. Rev.* **D97** (2018) 012004, [[arXiv:1709.00129](#)].
- [7] **LHCb** Collaboration, R. Aaij et al., *Measurement of the ratio of branching fractions $\mathcal{B}(\bar{B}^0 \rightarrow D^{*+}\tau^-\bar{\nu}_\tau)/\mathcal{B}(\bar{B}^0 \rightarrow D^{*+}\mu^-\bar{\nu}_\mu)$* , *Phys. Rev. Lett.* **115** (2015) 111803, [[arXiv:1506.08614](#)]. [Erratum: *Phys. Rev. Lett.* **115** (2015) 159901].
- [8] **LHCb** Collaboration, R. Aaij et al., *Test of Lepton Flavor Universality by the measurement of the $B^0 \rightarrow D^{*-}\tau^+\nu_\tau$ branching fraction using three-prong τ decays*, *Phys. Rev.* **D97** (2018) 072013, [[arXiv:1711.02505](#)].
- [9] **LHCb** Collaboration, R. Aaij et al., *Measurement of the ratio of the $B^0 \rightarrow D^{*-}\tau^+\nu_\tau$ and $B^0 \rightarrow D^{*-}\mu^+\nu_\mu$ branching fractions using three-prong τ -lepton decays*, *Phys. Rev. Lett.* **120** (2018) 171802, [[arXiv:1708.08856](#)].

- [10] **Belle** Collaboration, A. Abdesselam et al., *Measurement of $\mathcal{R}(D)$ and $\mathcal{R}(D^*)$ with a semileptonic tagging method*, [arXiv:1904.08794](#).
- [11] **HFLAV** Collaboration, Y. Amhis et al., *Averages of b -hadron, c -hadron, and τ -lepton properties as of summer 2016*, *Eur. Phys. J. C* **77** (2017) 895, [[arXiv:1612.07233](#)].
- [12] S. Fajfer, J. F. Kamenik, and I. Nisandzic, *On the $B \rightarrow D^* \tau \bar{\nu}_\tau$ Sensitivity to New Physics*, *Phys. Rev.* **D85** (2012) 094025, [[arXiv:1203.2654](#)].
- [13] P. Biancofiore, P. Colangelo, and F. De Fazio, *On the anomalous enhancement observed in $B \rightarrow D^{(*)} \tau \bar{\nu}_\tau$ decays*, *Phys. Rev.* **D87** (2013) 074010, [[arXiv:1302.1042](#)].
- [14] **LHCb** Collaboration, R. Aaij et al., *Measurement of the ratio of branching fractions $\mathcal{B}(B_c^+ \rightarrow J/\psi \tau^+ \nu_\tau)/\mathcal{B}(B_c^+ \rightarrow J/\psi \mu^+ \nu_\mu)$* , *Phys. Rev. Lett.* **120** (2018) 121801, [[arXiv:1711.05623](#)].
- [15] R. Dutta and A. Bhol, *$B_c \rightarrow (J/\psi, \eta_c) \tau \nu$ semileptonic decays within the standard model and beyond*, *Phys. Rev.* **D96** (2017) 076001, [[arXiv:1701.08598](#)].
- [16] R. Watanabe, *New Physics effect on $B_c \rightarrow J/\psi \tau \bar{\nu}$ in relation to the $R_{D^{(*)}}$ anomaly*, *Phys. Lett.* **B776** (2018) 5, [[arXiv:1709.08644](#)].
- [17] C.-T. Tran, M. A. Ivanov, J. G. Krner, and P. Santorelli, *Implications of new physics in the decays $B_c \rightarrow (J/\psi, \eta_c) \tau \nu$* , *Phys. Rev.* **D97** (2018) 054014, [[arXiv:1801.06927](#)].
- [18] **LHCb** Collaboration, R. Aaij et al., *Search for lepton-universality violation in $B^+ \rightarrow K^+ \ell^+ \ell^-$ decays*, [arXiv:1903.09252](#).
- [19] **LHCb** Collaboration, R. Aaij et al., *Test of lepton universality with $B^0 \rightarrow K^{*0} \ell^+ \ell^-$ decays*, *JHEP* **08** (2017) 055, [[arXiv:1705.05802](#)].
- [20] **Belle** Collaboration, A. Abdesselam et al., *Test of lepton flavor universality in $B \rightarrow K^* \ell^+ \ell^-$ decays at Belle*, [arXiv:1904.02440](#).
- [21] S. Bifani, S. Descotes-Genon, A. Romero Vidal, and M.-H. Schune, *Review of Lepton Universality tests in B decays*, *J. Phys.* **G46** (2019) 023001, [[arXiv:1809.06229](#)].
- [22] **LHCb** Collaboration, R. Aaij et al., *Measurement of Form-Factor-Independent Observables in the Decay $B^0 \rightarrow K^{*0} \mu^+ \mu^-$* , *Phys. Rev. Lett.* **111** (2013) 191801, [[arXiv:1308.1707](#)].
- [23] **LHCb** Collaboration, R. Aaij et al., *Angular analysis of the $B^0 \rightarrow K^{*0} \mu^+ \mu^-$ decay using 3 fb^{-1} of integrated luminosity*, *JHEP* **02** (2016) 104, [[arXiv:1512.04442](#)].
- [24] **LHCb** Collaboration, R. Aaij et al., *Angular analysis and differential branching fraction of the decay $B_s^0 \rightarrow \phi \mu^+ \mu^-$* , *JHEP* **09** (2015) 179, [[arXiv:1506.08777](#)].
- [25] **BaBar** Collaboration, J. P. Lees et al., *A test of heavy quark effective theory using a four-dimensional angular analysis of $\bar{B} \rightarrow D^* \ell^- \bar{\nu}_\ell$* , [arXiv:1903.10002](#).

- [26] Belle Collaboration, A. Abdesselam et al., *Measurement of CKM Matrix Element $|V_{cb}|$ from $\bar{B} \rightarrow D^{*+} \ell^- \bar{\nu}_\ell$* , [arXiv:1809.03290](#).
- [27] S. Jaiswal, S. Nandi, and S. K. Patra, *Extraction of $|V_{cb}|$ from $B \rightarrow D^{(*)} \ell \nu_\ell$ and the Standard Model predictions of $R(D^{(*)})$* , *JHEP* **12** (2017) 060, [[arXiv:1707.09977](#)].
- [28] D. Bigi, P. Gambino, and S. Schacht, *A fresh look at the determination of $|V_{cb}|$ from $B \rightarrow D^* \ell \nu$* , *Phys. Lett.* **B769** (2017) 441, [[arXiv:1703.06124](#)].
- [29] B. Grinstein and A. Kobach, *Model-Independent Extraction of $|V_{cb}|$ from $\bar{B} \rightarrow D^* \ell \bar{\nu}$* , *Phys. Lett.* **B771** (2017) 359, [[arXiv:1703.08170](#)].
- [30] P. Gambino, M. Jung, and S. Schacht, *The V_{cb} puzzle: an update*, [arXiv:1905.08209](#).
- [31] P. Colangelo and F. De Fazio, *Tension in the inclusive versus exclusive determinations of $|V_{cb}|$: a possible role of new physics*, *Phys. Rev.* **D95** (2017) 011701, [[arXiv:1611.07387](#)].
- [32] P. Colangelo and F. De Fazio, *Scrutinizing $\bar{B} \rightarrow D^* (D\pi) \ell^- \bar{\nu}_\ell$ and $\bar{B} \rightarrow D^* (D\gamma) \ell^- \bar{\nu}_\ell$ in search of new physics footprints*, *JHEP* **06** (2018) 082, [[arXiv:1801.10468](#)].
- [33] R. Alonso, A. Kobach, and J. Martin Camalich, *New physics in the kinematic distributions of $\bar{B} \rightarrow D^{(*)} \tau^- (\rightarrow \ell^- \bar{\nu}_\ell \nu_\tau) \bar{\nu}_\tau$* , *Phys. Rev.* **D94** (2016) 094021, [[arXiv:1602.07671](#)].
- [34] D. Becirevic, S. Fajfer, I. Nisandzic, and A. Tayduganov, *Angular distributions of $\bar{B} \rightarrow D^{(*)} \ell \bar{\nu}_\ell$ decays and search of New Physics*, [arXiv:1602.03030](#).
- [35] Z. Ligeti, M. Papucci, and D. J. Robinson, *New Physics in the Visible Final States of $B \rightarrow D^{(*)} \tau \nu$* , *JHEP* **01** (2017) 083, [[arXiv:1610.02045](#)].
- [36] A. K. Alok, D. Kumar, S. Kumbhakar, and S. U. Sankar, *D^* polarization as a probe to discriminate new physics in $\bar{B} \rightarrow D^* \tau \bar{\nu}$* , *Phys. Rev.* **D95** (2017) 115038, [[arXiv:1606.03164](#)].
- [37] C.-H. Chen and S.-h. Nam, *Left-right mixing on leptonic and semileptonic $b \rightarrow u$ decays*, *Phys. Lett.* **B666** (2008) 462–466, [[arXiv:0807.0896](#)].
- [38] A. J. Buras, K. Gemmler, and G. Isidori, *Quark flavour mixing with right-handed currents: an effective theory approach*, *Nucl. Phys.* **B843** (2011) 107, [[arXiv:1007.1993](#)].
- [39] A. Crivellin, *Effects of right-handed charged currents on the determinations of $|V(ub)|$ and $|V(cb)|$* , *Phys. Rev.* **D81** (2010) 031301, [[arXiv:0907.2461](#)].
- [40] A. Crivellin and S. Pokorski, *Can the differences in the determinations of V_{ub} and V_{cb} be explained by New Physics?*, *Phys. Rev. Lett.* **114** (2015) 011802, [[arXiv:1407.1320](#)].
- [41] F. U. Bernlochner, Z. Ligeti, and S. Turczyk, *New ways to search for right-handed current in $B \rightarrow \rho \ell \bar{\nu}$ decay*, *Phys. Rev.* **D90** (2014) 094003, [[arXiv:1408.2516](#)].

- [42] F. U. Bernlochner, $B \rightarrow \pi\tau\bar{\nu}_\tau$ decay in the context of type II 2HDM, *Phys. Rev.* **D92** (2015) 115019, [[arXiv:1509.06938](#)].
- [43] M. Blanke, A. Crivellin, S. de Boer, M. Moscati, U. Nierste, I. Nisandzic, and T. Kitahara, *Impact of polarization observables and $B_c \rightarrow \tau\nu$ on new physics explanations of the $b \rightarrow c\tau\nu$ anomaly*, *Phys. Rev.* **D99** (2019) 075006, [[arXiv:1811.09603](#)].
- [44] M. Blanke, A. Crivellin, T. Kitahara, M. Moscati, U. Nierste, and I. Nisandzic, *Addendum: "Impact of polarization observables and $B_c \rightarrow \tau\nu$ on new physics explanations of the $b \rightarrow c\tau\nu$ anomaly"*, [arXiv:1905.08253](#).
- [45] G. Banelli, R. Fleischer, R. Jaarsma, and G. Tetlalmatzi-Xolocotzi, *Decoding (Pseudo)-Scalar Operators in Leptonic and Semileptonic B Decays*, *Eur. Phys. J.* **C78** (2018) 911, [[arXiv:1809.09051](#)].
- [46] W. Buchmuller and D. Wyler, *Effective Lagrangian Analysis of New Interactions and Flavor Conservation*, *Nucl. Phys.* **B268** (1986) 621.
- [47] V. Cirigliano, J. Jenkins, and M. Gonzalez-Alonso, *Semileptonic decays of light quarks beyond the Standard Model*, *Nucl. Phys.* **B830** (2010) 95, [[arXiv:0908.1754](#)].
- [48] M. Jung and D. M. Straub, *Constraining new physics in $b \rightarrow c\ell\nu$ transitions*, *JHEP* **01** (2019) 009, [[arXiv:1801.01112](#)].
- [49] A. Celis, M. Jung, X.-Q. Li, and A. Pich, *Scalar contributions to $b \rightarrow c(u)\tau\nu$ transitions*, *Phys. Lett.* **B771** (2017) 168, [[arXiv:1612.07757](#)].
- [50] J. Charles, A. Le Yaouanc, L. Oliver, O. Pene, and J. C. Raynal, *Heavy to light form-factors in the heavy mass to large energy limit of QCD*, *Phys. Rev.* **D60** (1999) 014001, [[hep-ph/9812358](#)].
- [51] M. Beneke and T. Feldmann, *Symmetry breaking corrections to heavy to light B meson form-factors at large recoil*, *Nucl. Phys.* **B592** (2001) 3, [[hep-ph/0008255](#)].
- [52] C. F. Uhlemann and N. Kauer, *Narrow-width approximation accuracy*, *Nucl. Phys.* **B814** (2009) 195, [[arXiv:0807.4112](#)].
- [53] C. L. Y. Lee, M. Lu, and M. B. Wise, *$B(l_4)$ and $D(l_4)$ decay*, *Phys. Rev.* **D46** (1992) 5040.
- [54] S. Faller, T. Feldmann, A. Khodjamirian, T. Mannel, and D. van Dyk, *Disentangling the Decay Observables in $B^- \rightarrow \pi^+\pi^-\ell^-\bar{\nu}_\ell$* , *Phys. Rev.* **D89** (2014) 014015, [[arXiv:1310.6660](#)].
- [55] X.-W. Kang, B. Kubis, C. Hanhart, and U.-G. Meiner, *B_{l4} decays and the extraction of $|V_{ub}|$* , *Phys. Rev.* **D89** (2014) 053015, [[arXiv:1312.1193](#)].
- [56] C. Hambrock and A. Khodjamirian, *Form factors in $\bar{B}^0 \rightarrow \pi\pi\ell\bar{\nu}_\ell$ from QCD light-cone sum rules*, *Nucl. Phys.* **B905** (2016) 373, [[arXiv:1511.02509](#)].

- [57] S. Cheng, A. Khodjamirian, and J. Virto, *B* \rightarrow $\pi\pi$ Form Factors from Light-Cone Sum Rules with B-meson Distribution Amplitudes, *JHEP* **05** (2017) 157, [[arXiv:1701.01633](#)].
- [58] S. Cheng, A. Khodjamirian, and J. Virto, *Timelike-helicity B* \rightarrow $\pi\pi$ form factor from light-cone sum rules with dipion distribution amplitudes, *Phys. Rev.* **D96** (2017), no. 5 051901, [[arXiv:1709.00173](#)].
- [59] **Particle Data Group** Collaboration, M. Tanabashi et al., *Review of Particle Physics*, *Phys. Rev.* **D98** (2018) 030001.
- [60] **Belle** Collaboration, A. Sibidanov et al., *Search for B* $^- \rightarrow \mu^- \bar{\nu}_\mu$ *Decays at the Belle Experiment*, *Phys. Rev. Lett.* **121** (2018) 031801, [[arXiv:1712.04123](#)].
- [61] **Belle** Collaboration, P. Hamer et al., *Search for B* $^0 \rightarrow \pi^- \tau^+ \nu_\tau$ *with hadronic tagging at Belle*, *Phys. Rev.* **D93** (2016) 032007, [[arXiv:1509.06521](#)].
- [62] I. Sentitemsu Imsong, A. Khodjamirian, T. Mannel, and D. van Dyk, *Extrapolation and unitarity bounds for the B* \rightarrow π *form factor*, *JHEP* **02** (2015) 126, [[arXiv:1409.7816](#)].
- [63] A. Khodjamirian and A. V. Rusov, *B_s $\rightarrow K\ell\nu_\ell$ and B_(s) $\rightarrow \pi(K)\ell^+\ell^-$ decays at large recoil and CKM matrix elements*, *JHEP* **08** (2017) 112, [[arXiv:1703.04765](#)].
- [64] **Flavour Lattice Averaging Group** Collaboration, S. Aoki et al., *FLAG Review 2019*, [arXiv:1902.08191](#).
- [65] A. Bharucha, D. M. Straub, and R. Zwicky, *B* $\rightarrow V\ell^+\ell^-$ *in the Standard Model from light-cone sum rules*, *JHEP* **08** (2016) 098, [[arXiv:1503.05534](#)].
- [66] P. Ball and R. Zwicky, *B_{d,s} $\rightarrow \rho, \omega, K^*, \phi$ decay form-factors from light-cone sum rules revisited*, *Phys. Rev.* **D71** (2005) 014029, [[hep-ph/0412079](#)].
- [67] D. Du, A. X. El-Khadra, S. Gottlieb, A. S. Kronfeld, J. Laiho, E. Lunghi, R. S. Van de Water, and R. Zhou, *Phenomenology of semileptonic B-meson decays with form factors from lattice QCD*, *Phys. Rev.* **D93** (2016) 034005, [[arXiv:1510.02349](#)].
- [68] R. Dutta and A. Bhol, *b* $\rightarrow (c, u), \tau\nu$ *leptonic and semileptonic decays within an effective field theory approach*, *Phys. Rev.* **D96** (2017) 036012, [[arXiv:1611.00231](#)].
- [69] S. Sahoo, A. Ray, and R. Mohanta, *Model independent investigation of rare semileptonic b* $\rightarrow u\bar{\nu}_l$ *decay processes*, *Phys. Rev.* **D96** (2017) 115017, [[arXiv:1711.10924](#)].
- [70] C.-H. Chen and T. Nomura, *Charged Higgs boson contribution to B_q $^- \rightarrow \ell\bar{\nu}$ and $\bar{B} \rightarrow (P, V)\ell\bar{\nu}$ in a generic two-Higgs doublet model*, *Phys. Rev.* **D98** (2018) 095007, [[arXiv:1803.00171](#)].
- [71] C.-H. Chen and C.-Q. Geng, *Charged Higgs on B* $^- \rightarrow \tau\bar{\nu}_\tau$ *and $\bar{B} \rightarrow P(V)\ell\bar{\nu}_\ell$* , *JHEP* **10** (2006) 053, [[hep-ph/0608166](#)].

- [72] **BaBar** Collaboration, B. Aubert et al., *Measurement of branching fractions of B decays to $K(1)(1270)\pi$ and $K(1)(1400)\pi$ and determination of the CKM angle α from $B^0 \rightarrow a(1)(1260)^+ \pi^-$, *Phys. Rev.* **D81** (2010) 052009, [[arXiv:0909.2171](#)].*
- [73] **Belle** Collaboration, J. Dalseno et al., *Measurement of Branching Fraction and First Evidence of CP Violation in $B^0 \rightarrow a_1^\pm(1260)\pi^\mp$ Decays*, *Phys. Rev.* **D86** (2012) 092012, [[arXiv:1205.5957](#)].
- [74] **BaBar, Belle** Collaboration, A. J. Bevan et al., *The Physics of the B Factories*, *Eur. Phys. J.* **C74** (2014) 3026, [[arXiv:1406.6311](#)].
- [75] D. Scora and N. Isgur, *Semileptonic meson decays in the quark model: An update*, *Phys. Rev.* **D52** (1995) 2783, [[hep-ph/9503486](#)].
- [76] A. Deandrea, R. Gatto, G. Nardulli, and A. D. Polosa, *Semileptonic $B \rightarrow \rho$ and $B \rightarrow a_1$ transitions in a quark - meson model*, *Phys. Rev.* **D59** (1999) 074012, [[hep-ph/9811259](#)].
- [77] T. M. Aliev and M. Savci, *Semileptonic $B \rightarrow a(1)$ lepton neutrino decay in QCD*, *Phys. Lett.* **B456** (1999) 256, [[hep-ph/9901395](#)].
- [78] H.-Y. Cheng, C.-K. Chua, and C.-W. Hwang, *Covariant light front approach for s wave and p wave mesons: Its application to decay constants and form-factors*, *Phys. Rev.* **D69** (2004) 074025, [[hep-ph/0310359](#)].
- [79] H.-Y. Cheng and K.-C. Yang, *Hadronic charmless B decays $B \rightarrow AP$* , *Phys. Rev.* **D76** (2007) 114020, [[arXiv:0709.0137](#)].
- [80] Z.-G. Wang, *Analysis of the $B \rightarrow a_1(1260)$ form-factors with light-cone QCD sum rules*, *Phys. Lett.* **B666** (2008) 477, [[arXiv:0804.0907](#)].
- [81] K.-C. Yang, *Form-Factors of $B(u,d,s)$ Decays into P -Wave Axial-Vector Mesons in the Light-Cone Sum Rule Approach*, *Phys. Rev.* **D78** (2008) 034018, [[arXiv:0807.1171](#)].
- [82] R.-H. Li, C.-D. Lu, and W. Wang, *Transition form factors of B decays into p -wave axial-vector mesons in the perturbative QCD approach*, *Phys. Rev.* **D79** (2009) 034014, [[arXiv:0901.0307](#)].
- [83] S. Momeni and R. Khosravi, *Semileptonic $B_{(s)} \rightarrow a_1(K_1)\ell^+\ell^-$ decays via the light-cone sum rules with B -meson distribution amplitudes*, *Phys. Rev.* **D96** (2017) 016018, [[arXiv:1804.04844](#)].
- [84] X.-W. Kang, T. Luo, Y. Zhang, L.-Y. Dai, and C. Wang, *Semileptonic B and B_s decays involving scalar and axial-vector mesons*, *Eur. Phys. J.* **C78** (2018) 909, [[arXiv:1808.02432](#)].
- [85] F. De Fazio, T. Feldmann, and T. Hurth, *Light-cone sum rules in soft-collinear effective theory*, *Nucl. Phys.* **B733** (2006) 1, [[hep-ph/0504088](#)]. [Erratum: *Nucl. Phys.* **B800** (2008) 405].

-
- [86] F. De Fazio, T. Feldmann, and T. Hurth, *SCET sum rules for $B \rightarrow P$ and $B \rightarrow V$ transition form factors*, *JHEP* **02** (2008) 031, [[arXiv:0711.3999](#)].
 - [87] A. Khodjamirian, T. Mannel, and N. Offen, *Form-factors from light-cone sum rules with B -meson distribution amplitudes*, *Phys. Rev.* **D75** (2007) 054013, [[hep-ph/0611193](#)].
 - [88] C. Bourrely, I. Caprini, and L. Lellouch, *Model-independent description of $B \rightarrow \pi \ell \nu$ decays and a determination of $|V_{ub}|$* , *Phys. Rev.* **D79** (2009) 013008, [[arXiv:0807.2722](#)]. [Erratum: *Phys. Rev.* **D82** (2010) 099902].